FLOW OF HEAT AND MASS TRANSFER IN MHD MICROPOLAR FLUID PAST STRETCHING PERMEABLE SURFACE IN A POROUS MEDIUM WITH SORET AND DUFOUR EFFECTS.

, Nigeria **E. O. Fatunmbi[1], S. S. Okoya[2], A. Adeniyan[3]**

[1]Department of Mathematics and Statistics, Federal Polytechnic, Ilaro.

[2-3]Department of Mathematics, University of Lagos. Akoka, Lagos

ABSTRACT

This article considers the flow, heat and mass transfer of steady, two dimensional, electrically conducting micropolar fluid over a vertically stretching permeable plate in a Darcy Forchheimer porous medium. The study is pivoted on investigating the combined effects of thermo-diffusion (Soret) and diffusion thermo (Dufour) on a thermally radiating and electrically conducting micropolar fluid with the influences of viscous dissipation, heat generation/absorption and chemical reaction of the first order. A uniform magnetic field of magnitude is applied normal to the plate. The governing nonlinear partial differential equations (PDEs) are transformed into a system of coupled nonlinear ordinary differential equations (ODEs) using Lie scaling group of transformations, which are then solved numerically subject to the boundary conditions by Runge-Kutta Fehlberg fourth fifth integration scheme alongside the shooting method. Comparisons are made with the previous studies and an agreement is found between the present study and the previous findings as a special case of the present work. The influences of different flow parameters on the velocity, microrotation, temperature and concentration are discussed and displayed both tabularly and graphically.

Keywords: Magnetohydrodynamic flow, Micropolar fluid, Lie scaling group and heat and mass transfer.

Introduction

The concept of micropolar fluid as a sub-class of simple micro-fluid was developed by Eringen (1964, 1966) while the constitutive equations for the model of thermo-micropolar fluids were also derived by Eringen (1972). These are fluids with microstructures which constitute a substantial generalization of the Navier-stokes model and open up a new field of potential application. By this theory, each element of the fluid is associated to two sets of degrees of freedom: (a) translatory degrees of freedom, giving rise to velocity, and (b) rotation and stretch allowing the particles to undergo independent intrinsic spins and homogeneous deformation (Eringen, 1972). The concept of micropolar fluid is used to explain the class of fluids that possess certain microscopic effects which arises from the local structure and micromotion of the fluid element. Such fluids include: polymeric suspensions, animal blood, liquid crystal and colloidal fluids. They are of a complex nature and individual fluid particles may be of different shape and may shrink and/or expand, occasionally changing shape and rotating independently of the rotational movement of the fluid (Lukaszewicz, 1999).

In the recent times, a number of researches have been done on micropolar fluids owing to its important applications in engineering and industrial activities in capturing the flow of colloidal fluids, suspension solutions, dental fluids, paints, animal blood, arterial and cervical blood,

extrusion of polymer fluids and the cooling of metallic plate in water bath (Rahman, 2009, Chen *et al.,* 2011, Zueco *et al*., 2014).

The flow over a heated stretching plate has many practical applications in industrial manufacturing processes such as, aerodynamics extrusion of plastic sheets, glass-fiber, production and polymer industries, hot rolling and wire drawing. Grubka and Bobba (1985) investigated the effect of power law surface temperature variation on the heat transfer characteristics of a continuous; linearly stretching surface. Hassan and El- Arabawy (2003) carried out analysis on the effect of suction and injection on the flow and heat transfer characteristics for a continuously moving plate in a micropolar fluid in the presence of radiation. Siddheshwar and Mahabaleshwar (2011) studied the analytical solution to the stretching sheet boundary layer flow of a MHD micropolar fluid. Kumar (2013) analyzed the steady two-dimensional laminar boundary layer flow of a viscous, incompressible, electrically conducting fluid past a stretching sheet with slip effect.

 The boundary layer concept in MHD micropolar fluids on different geometries, subject to various boundary conditions have been studied by researchers. (Hassanien *et al., 1999;* Uddin, 2011). The important applications of such study are found in many engineering processes such as MHD generators, geothermal energy extractions and nuclear reactors. Khedr *et al*, (2009) considered MHD flow of a micropolar fluid along a vertical semi-infinite permeable plate in the presence of wall suction or injection effects and heat generation or absorption effects. (Pal and Chatterjee, 2010, Mahmoud, 2011).

Also, combined heat and mass transfer (or double-diffusion) in MHD micropolar fluid embedded in a saturated porous media has gained the attention of many researchers due to the effect of magnetic fields on flow control and on the performance of many system using electrically conducting fluids which is applicable in variety of engineering process such as, heat exchanger devices; chemical process industries such as, food processing and polymer production, petroleum reservoirs; geophysical engineering such as, moisture migration in fibrous insulation and nuclear waste due to temperature and concentration gradients. Makinde (2010), considered the MHD heat and mass transfer over a moving vertical plate with a convective surface boundary condition. Kumar, (2009) studied heat and mass transfer in a hydromagnetic flow of a micropolar fluid past a stretching sheet with surface condition parameter using finite element technique. Qasim *et al*., (2013) considered the problem with Newtonian heating and using Runge-Kutta Fehlberg fourth-fifth order method. Olajuwon *et al.,* (2014) investigated heat and mass transfer in a hydromagnetic flow of a micropolar fluid over a porous medium using Boussinesq model in the presence of uniform magnetic field, the governing equations were solved analytically using perturbation techniques. Mohammed and Abo-Dahab (2009) studied the influences of chemical reaction and thermal radiation on the heat and mass transfer MHD micropolar flow over a vertical moving porous plate in a porous medium with heat generation

The simultaneous occurrence of heat and mass transfer in a moving fluid could make the relations between the fluxes and the driving potentials of a more intricate nature; it has been observed that energy flux can be generated not only by temperature gradients but also by composition gradient, this fact is known as diffusion- thermo or Dufour effect. Likewise, mass fluxes can also be caused by temperature gradients and this is referred to as thermo-diffusion or Soret effect. In many reported studies the Dufour and Soret effects were neglected due to the fact that they are of smaller magnitude then those described by Fourier's and Fick's laws. However, such effects are important when the density difference exists in the flow regimes, for instance, the Soret effects has be utilized for isotope separation. Dufour effect was found to be of considerable magnitude in a mixture between gases with considerable very light molecular   weight (e.g.,H_2 & H_e) and medium molecular weight (e.g.,N_2 & Air) (Eckert and Drake, 1972, Nawaz, *et al*., 2012)). The accurate description of velocity, temperature and concentration at the wall is not possible by neglecting Soret, Dufour and other important parameters. Srinivasacharya and RamReddy

(2011) considered Soret and Dufour effects on mixed convection in a non-Darcy micropolar fluid, the problem was later extended to include the influence of magnetic field by Srinivasacharya and Upendar (2013). Osalusi *et al*., (2008) investigated the effects of Soret and Dufour on combined heat and mass transfer on MHD flow of viscous fluid. Pal and Chatterjee (2010) studied the steady two dimensional mixed convection and mass transfer flow past semi-infinite vertical porous plate embedded in a micropolar fluids-saturated porous medium taking into account the Soret and Dufour effects in the presence of thermal radiation, Ohmic dissipation and inertia effects. Afify (2009) studied MHD free convective heat and mass transfer over a stretching sheet with the effects of thermo-diffusion and diffusion-thermo, in the presence of suction/injection using scaling transformations to reduce the nonlinear PDEs governing the flow to ODEs with the appropriate boundary condition, and then solved with fourth order Runge Kutta integration scheme with shooting method. Subhakar and Gangadhar (2012) investigated the combined effects of the free convective heat and mass transfer on the unsteady two dimensional boundary layer flow over a stretching vertical plate in the presence of heat generation/absorption, Soret and Dufour effects.

The effect of chemical reactions on the transport of chemical reacting species need to be included in the mass transfer analysis. Nawaz *et al., (2012),* considered Soret and Dufour effects on MHD flow of viscous fluid between a radially stretching sheets with first order chemical reaction.

Researchers have developed and renewed interest in the flows induced by stretching surfaces with Soret and Dufour effects due to their significant applications in areas such as hydrology, geosciences and petrology. However, literature survey shows that no attention has been given to the study of combined effects of Soret and Dufour on steady MHD micropolar fluid flow past vertical stretching plates inspite of their much importance. The aim of this study therefore, is to investigate the combined effects of Soret and Dufour on heat and mass transfer flow of an electrically conducting micropolar fluid past a vertical permeable stretching plate in a porous medium with thermal radiation, viscous dissipation, non-uniform heat source/sink and first order chemical reaction.

Flow analysis

The stress tensor and couple stress tensor relations for isotropic micropolar fluid as given by (Eringen, 1966; Lukaszewicz, 1999, Chen *et al.2011*):

$$\tau_{ij} = \left(-p + \lambda v_k,_k\right)\delta_{ij} + \mu\left(v_{i,j} + v_{j,i}\right) + \mu_r\left(v_{j,i} - v_{i,j}\right) - 2\mu_r \in_{kij} \omega_k \quad (1)$$

$$C_{ij} = c_o\omega_{k,k}\delta_{ij} + c_d\left(\omega_{i,j} + \omega_{j,i}\right) + c_a\left(\omega_{j,i} - \omega_{i,j}\right). \quad (2)$$

Here, $(i, j, k = 1,2,3)$. Also τ_{ij} or ($\boldsymbol{\tau}$) is anti-symmetric Cauchy stress tensor or matrix (unlike Newtonian fluid), p is the pressure, λ, μ are the usual viscosity coefficients or the second viscosity coefficient and dynamic viscosity respectively, μ_r is the dynamic microrotation viscosity, c_O, c_a and c_d are the coefficients of angular viscosity. v_i is the velocity component, ω_k is the angular velocity component, $\in_{kij}$ is the alternating/permutation stress tensor, C_{ij} or ($\mathbf{C}$) is the couple stress tensor or matrix, δ_{ij} is the usual Kronecker delta, $v_{i,j} = \dfrac{\partial v_i}{\partial x_j}$ & $\omega_{i,j} = \dfrac{\partial \omega_i}{\partial x_j}$ are the partial derivatives with respect to coordinates $\left(x_1, x_2, x_3\right)$. The following inequalities must hold in order that eqns. (1) & (2) remain valid:

$$\mu \geq 0, \ 3\lambda + 2\mu \geq 0, \ \mu_r \geq 0. \quad (3)$$

Flow, heat and mass transfer transport equations

The constitutive equations of micropolar fluid flows, heat and mass transfer derivable from (1)-(2) are stated respectively as conservation laws of, mass, momentum, angular momentum, energy and mass diffusion (Lukaszewicz, 1999; Jaluria, 1980; Vafai, 2005):

Mass conservation (Continuity) equation

$$\frac{D\rho}{Dt} + \rho\nabla\cdot\mathbf{V} = 0$$

(4)

Momentum equation

$$\rho\frac{D\mathbf{V}}{Dt} = \nabla\cdot\boldsymbol{\tau} + \rho\mathbf{f}$$

(5)

Angular momentum (Microrotation) equation

$$\rho j\frac{D\boldsymbol{\omega}}{Dt} = \nabla\cdot\boldsymbol{C} + \rho\boldsymbol{g} + \boldsymbol{\tau_x}$$

(6)

Energy equation

$$\rho C_p\frac{DT}{Dt} = -\nabla\cdot\mathbf{q} + \boldsymbol{\tau}:(\nabla\mathbf{V}) + \mathbf{C}:(\nabla\boldsymbol{\omega}) - \boldsymbol{\tau_x}\cdot\boldsymbol{\omega} + q''' - \nabla\cdot\mathbf{q_r} + Dm\frac{K_T\nabla^2 C}{CsCp}$$

(7)

Species concentration (Mass diffusion) equation

$$\frac{DC}{Dt} = \nabla\cdot(Dm\nabla C) + Dm\frac{K_T}{T_m}\nabla^2 T - k_r(C - C_\infty)$$

(8)

where ":" is the dyadic product operator and "·" stands for the usual vector product. In addition, $\frac{D}{Dt} = \frac{\partial}{\partial t} + \mathbf{V}\cdot\nabla$ is the material derivative, $\frac{\partial}{\partial t}$ is the local rate while $\mathbf{V}\cdot\nabla$ is the operator convective part, and $\nabla = \left(\frac{\partial}{\partial x_1}, \frac{\partial}{\partial x_2}, \frac{\partial}{\partial x_3}\right)$ is the Hamiltonian operator. Also ρ is the micropolar fluid density, j is the micro inertial density, $\mathbf{V}$ is the velocity vector, $\mathbf{f}$ is the body force per unit mass, $\boldsymbol{g}$ is the body torque per unit mass, $\boldsymbol{\tau_x}$ is the force arising from anti-symmetric (skew-symmetric) part of the stress tensor, Dm is the coefficient of mass diffusivity, Cs is the fluid susceptibility and C is the species concentration, T and T_m are the micropolar fluid temperature and mean fluid temperatures respectively, K_T is the thermal diffusion ratio, k_r is the constant rate of homogeneous chemical reaction. The specific heat at constant pressure is Cp, q''' is the non-uniform heat source/sink, $\mathbf{q}$ is the heat flux vector, whereas $\mathbf{q_r}$ is the radiative heat flux vector.

The relevant Maxwell equations under MHD approximations are:

$$\nabla\cdot\mathbf{E} = 0 \qquad\qquad (9)$$

$$\nabla\cdot\mathbf{J} = 0 \qquad\qquad (10)$$

$$\nabla\cdot\mathbf{B} = 0 \qquad\qquad (11)$$

$$\nabla\wedge\mathbf{E} = -\frac{\partial\mathbf{B}}{\partial t} \qquad\qquad (12)$$

$$\nabla\wedge\mathbf{B} = \mu_e\mathbf{J} \qquad\qquad (13)$$

$$\mathbf{J} = \sigma \left(\mathbf{E} + \mathbf{V} \wedge \mathbf{B} - \beta \mathbf{J} \wedge \mathbf{B} \right) \qquad (14)$$

Here, $\mathbf{E}$, $\mathbf{J}$, $\mathbf{B}$, $\mathbf{V}$, μ_e, σ, β and t are respectively the electric field intensity, the current density, magnetic field induction (strength), fluid velocity, magnetic permeability of the medium, electric conductivity of micropolar fluid, Hall factor and time variable.

Basic assumptions of the flow.

The following assumptions are made in this study:

(i)   The flow is assumed to be two-dimensional with $\bar{z}$ axis taken along the stretching surface in the flow direction and $\bar{y}$-axis is perpendicular to it.

(ii)   A uniform magnetic field of strength B_o is applied normal to the flow direction.

(iii)   The magnetic Reynolds number of the flow is taken to be small enough so that the induced magnetic field is negligible and that the influence of Hall currents with ion-slips is negligible.

(iv)   The fluid physical properties are assumed to be constant except for the density variation in the body force term of the momentum equations (Boussinesq approximation).

(v)   The fluid is assumed to be a gray, emitting and absorbing, but not scattering medium and the optically thick radiation heat flux is simplified using the Rosseland approximation.

(vi)   It is assumed that the radiative heat flux in $\bar{z}$-direction is negligible compared to that in the $\bar{y}$-direction.

(vii)   The wall velocity is $\bar{w} = w_w = a_1 \bar{z}$, and the velocity upstream is assumed to be zero.

(viii) Diffusion-thermo and thermo-diffusion effects are also considered.

(ix)   The corresponding components of velocity are $(0, \bar{v}, \bar{w})$ for coordinates $(\bar{x}, \bar{y}, \bar{z})$.

(x)   A chemical species diffuses into the ambient fluid initiating an irreversible homogeneous chemical reaction of order 1 with a constant rate k_r.

(xi)   The plate is subjected to prescribed power law temperature at the wall and the presence of uniform surface suction /injection.
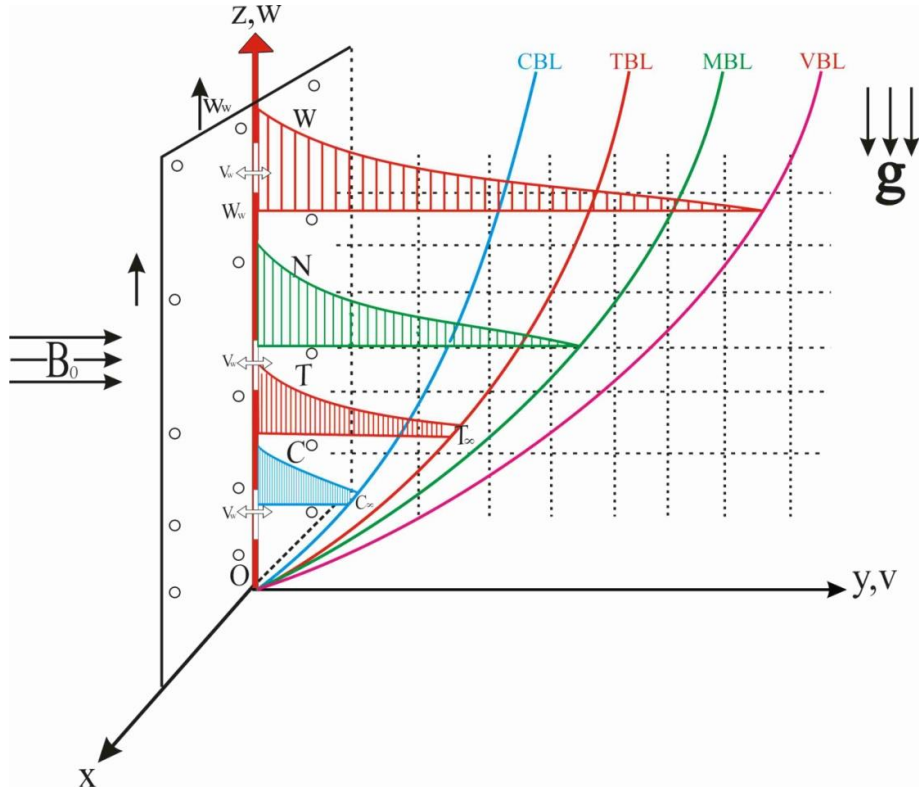
Fig.1 Geometry of the flow.

Under the above assumptions and boundary layer approximation, the governing boundary layer equations of the flow are:

Continuity equation:

$$\frac{\partial \overline{v}}{\partial \overline{y}} + \frac{\partial \overline{w}}{\partial \overline{z}} = 0$$

(15)

Momentum equation:

$$\overline{v}\frac{\partial \overline{w}}{\partial \overline{y}} + \overline{w}\frac{\partial \overline{w}}{\partial \overline{z}} = \frac{(\mu+\kappa)}{\rho}\frac{\partial^2 \overline{w}}{\partial \overline{y}^2} + \frac{\kappa}{\rho}\frac{\partial \overline{N}}{\partial \overline{y}} + g\beta_T\left(T-T_\infty\right) + g\beta_c\left(C-C_\infty\right) - \frac{\upsilon\overline{w}}{K_p} - \frac{F\overline{w}^2}{K_p} - \frac{\sigma B_0^2 \overline{w}}{\rho}$$

(16)

Angular momentum (Microrotation):

$$\overline{v}\frac{\partial \overline{N}}{\partial \overline{y}} + \overline{w}\frac{\partial \overline{N}}{\partial \overline{z}} = \frac{\gamma}{\rho_j}\frac{\partial^2 \overline{N}}{\partial \overline{y}^2} - \frac{\kappa}{\rho_j}\left(2\overline{N} + \frac{\partial \overline{w}}{\partial \overline{y}}\right)$$

(17)

Energy equation:

$$\overline{v}\frac{\partial T}{\partial \overline{y}} + \overline{w}\frac{\partial T}{\partial \overline{z}} = \frac{k}{\rho Cp}\frac{\partial^2 T}{\partial \overline{y}^2} + \frac{\mu+\kappa}{\rho Cp}\left(\frac{\partial \overline{w}}{\partial \overline{y}}\right)^2 - \frac{1}{\rho Cp}\frac{\partial q_r}{\partial \overline{y}} + \frac{q'''}{\rho Cp} + \frac{D_m K_T}{Cs Cp}\frac{\partial^2 C}{\partial \overline{y}^2}.$$

(18)

Species concentration (Mass diffusion) equation:

$$\bar{v}\frac{\partial C}{\partial \bar{y}} + \bar{w}\frac{\partial C}{\partial \bar{z}} = Dm\frac{\partial^2 C}{\partial \bar{y}^2} + \frac{DmK_T}{T_m}\frac{\partial^2 T}{\partial \bar{y}^2} - k_r(C - C_\infty).$$

(19)

The associated boundary conditions are:

$$\bar{y} = 0: \bar{w} = w_w = a_1\bar{z}, \ \bar{v} = v_w(z), \ \bar{N} = -m\frac{\partial \bar{w}}{\partial \bar{y}} \ , T = T_w = T_\infty + A\bar{z}^n \ C = C_w = C_\infty + B\bar{z}^q$$

$$y \to \infty: \ \bar{w} \to 0, \ \bar{N} = 0, \ T \to T_\infty, \ C \to C_\infty.$$

(20)

Where $\bar{z}$ and $\bar{y}$ are the dimensional Cartesian coordinate along and normal to the plate respectively, $\bar{w}$ and $\bar{v}$ are the dimensional velocity components along $\bar{z}$ and $\bar{y}$ direction respectively, μ is the dynamic viscosity, κ is the vortex viscosity, $\bar{N}$ is the dimensional microrotation vector, ρ is the fluid density, j is the micro-inertia density, γ is the spin gradient viscosity, υ is kinematic viscosity, k is thermal conductivity, T is the fluid temperature, C is the concentration, g is the acceleration due to gravity, β_T is the coefficient of thermal expansion, β_c is the coefficient of concentration expansion, k_r is the constant rate of chemical reaction, Dm is the mass diffusivity, K_p is the permeability of the porous medium, F is the Forchheimer c onstant, T_m is the mean fluid temperature, Cp is the specific heat capacity at constant temperature, q''' is the non-uniform heat source/sink, B_0 is the magnetic field strength, v_w is the suction/injection velocity, A and B and a_1 are constants, p is the variable wall temperature, q is variable mass concentration, m is also a constant and $0 \le m \le 1$, the case when $m = 0$ indicates that $N = 0$ and represents strong concentration of micro elements in which the micro elements close to the wall surface are unable to rotate (Guram & Smith, 1980). The case $m = \frac{1}{2}$ indicates the vanishing of the anti-symmetric stress tensor and represents weak concentration of micro elements (Ahmadi, 1976). The case $m = 1$ is used for modelling of turbulent boundary layer flows (Peddieson, 1972). In this study we consider only the case $m = \frac{1}{2}$. Also, $n, q, T_w, C_w, T_\infty, C_\infty$ is the temperature parameter, concentration parameter, wall temperature, wall concentration, free stream temperature and concentration respectively.

q_r is the radiative heat flux which is modelled as (Rosseland, 1936):

$$q_r = -\left(\frac{4\sigma * }{3\alpha *}\frac{\partial T^4}{\partial y}\right).$$

(21)   Where, $\sigma *$ is the Boltzmann constant and $\alpha *$ is the mean absorption coefficient. Assuming that the temperature difference can be expressed as a linear combination of the temperature such that T^4 can be expanded in Taylor series, i.e.

$$T^4 = T^4_\infty + 4T^3_\infty(T - T_\infty) + 6T^2_\infty(T - T_\infty)^2 + ...$$
$$T^4 \approx 4T^3_\infty T - 3T^4_\infty \quad \Rightarrow \quad \partial T^4 = 4T^3_\infty \partial T$$

(22) Therefore,

$$\frac{\partial q_r}{\partial y} = -\left(\frac{16\sigma * T^3_\infty}{3\alpha *}\frac{\partial^2 T}{\partial y^2}\right).$$

(23) q''' is the non-uniform heat source/sink given in the form (Pal and Chatterjee, 2010):

$$q''' = \frac{k W_{w(z)}}{z \upsilon}[A_1(T_w - T_\infty)\frac{\bar{w}}{w_w} + B_1(T - T_\infty)].$$

(24)

Here, A_1 and B_1 are coefficients of space and temperature dependent heat source\sink respectively, k is the thermal conductivity, υ is the kinematic viscosity, and w_w is the velocity of the stretching wall.

Introducing the following dimensionless quantities into Eqs. (15-20), to get the dimensionless governing equations (Uddin *et al, 2015*).

$$z = \frac{\bar{z}}{L}, \ y = \frac{\bar{y}}{L}\sqrt{Re}, \ w = \frac{\bar{w}}{w_w}, \ v = \frac{\bar{v}}{w_w}\sqrt{Re},$$

$$N = \frac{\bar{N}}{w_w\sqrt{Re}}L, \ \theta = \frac{T - T_\infty}{T_W - T_\infty}, \phi = \frac{C - C_\infty}{C_W - C_\infty}, Re = \frac{w_w L}{\upsilon} \qquad \frac{\partial v}{\partial y} + \frac{\partial w}{\partial z} = 0.$$

(25)

$$v\frac{\partial w}{\partial y} + w\frac{\partial w}{\partial z} = (1 + K)\frac{\partial^2 w}{\partial y^2} + K\frac{\partial N}{\partial y} + Gr\,\theta + Gc\,\phi - Daw - Fs\,w^2 - Mw.$$

(26)

$$v\frac{\partial N}{\partial y} + w\frac{\partial N}{\partial z} = \lambda\frac{\partial^2 N}{\partial y^2} - I\left(2N + \frac{\partial w}{\partial y}\right).$$

(27)

$$v\frac{\partial \theta}{\partial y} + w\left(p\frac{\theta}{z} + \frac{\partial \theta}{\partial z}\right) = \frac{1}{Pr}\left(1 + \frac{4}{3}R\right)\frac{\partial^2 \theta}{\partial y^2} + Ec(1 + K)\left(\frac{\partial w}{\partial y}\right)^2 + Du\frac{\partial^2 \phi}{\partial y^2} + \frac{1}{Pr}(A_1 w + B_1 \theta)$$

(28)

$$v\frac{\partial \phi}{\partial y} + w\left(q\frac{\phi}{z} + \frac{\partial \phi}{\partial z}\right) = \frac{1}{Sc}\frac{\partial^2 \phi}{\partial y^2} + Sr\frac{\partial^2 \theta}{\partial y^2} - \gamma_1 \phi.$$

(29)

$$y = 0: w = z, v = -f_w, \ N = -m\frac{\partial w}{\partial y}, \ \theta = z^p, \phi = z^q$$

$$y \to \infty: \ w \to 0, \ N = 0, T \to T_\infty, C \to C_\infty.$$

(30)

Where, $K = \frac{\kappa}{\mu}$ is the material (micropolar) parameter, $Gr = \frac{g\beta_T(T_w - T_\infty)}{w_w^2}L$ is the Grashof number, $Gc = \frac{g\beta c(C_w - C_\infty)}{w_w^2}L$ is the solutal Grashof number, $Da = \frac{\upsilon L}{k_p w_w}$ is the Darcy number, $Fs = \frac{LF}{k_p}$ is the Forchheimer number, $M = \frac{\sigma B_o^2 L}{w_w \rho}$ is the magnetic parameter, $\lambda = \frac{\gamma}{\upsilon \rho_j}$ is the microrotation density parameter, $I = \frac{kL}{w_w \rho_j}$ is the vortex viscosity parameter, $Pr = \frac{\mu Cp}{k}$ is the Prandtl number, $Ec = \frac{w_w^2}{Cp(T_w - T_\infty)}$ is the Eckert number, $Du = \frac{D_m K_T}{CsCp\upsilon}\frac{(C_w - C_\infty)}{(T_w - T_\infty)}$ is the Dufour number, $R = \frac{4\sigma^* T_\infty^3}{\alpha^* k_\infty}$ is the radiation parameter,

$Sc = \dfrac{\upsilon}{Dm}$ is the Schmidt number, $Sr = \dfrac{DmK_T}{T_m\upsilon}\dfrac{(T_w - T_\infty)}{(C_w - C_\infty)}$ is the Soret number, $\gamma_1 = \dfrac{k_r L}{w_w}$ is

the chemical reaction parameter of order 1, $\dfrac{v_w\sqrt{\mathrm{Re}}}{w_w} = -f_{w,}$ is the suction/injection parameter.

On introducing the stream function ψ defined as:

$$w = \frac{\partial \psi}{\partial y}, \quad v = -\frac{\partial \psi}{\partial z}.$$

(31)

Eqs. (26- 30) yield the following:

$$\frac{\partial \psi}{\partial y}\frac{\partial^2 \psi}{\partial z \partial y} - \frac{\partial \psi}{\partial z}\frac{\partial^2 \psi}{\partial y^2} = (1+K)\frac{\partial^3 \psi}{\partial y^3} + K\frac{\partial N}{\partial y} + Gr\,\theta + Gc\,\phi - Da\frac{\partial \psi}{\partial y} - Fs\left(\frac{\partial \psi}{\partial y}\right)^2 - M\frac{\partial \psi}{\partial y}.$$

(32)
$$\frac{\partial \psi}{\partial y}\frac{\partial N}{\partial z} - \frac{\partial \psi}{\partial z}\frac{\partial N}{\partial y} = \lambda\frac{\partial^2 N}{\partial y^2} - I\left(2N + \frac{\partial^2 \psi}{\partial y^2}\right).$$

(33)

$$\frac{\partial \psi}{\partial y}\left(p\frac{\theta}{z} + \frac{\partial \theta}{\partial z}\right) - \frac{\partial \psi}{\partial z}\frac{\partial \theta}{\partial y} = \frac{1}{\Pr}\left(1 + \frac{4}{3}R\right)\frac{\partial^2 \theta}{\partial y^2} + Ec(1+K)\left(\frac{\partial^2 \psi}{\partial y^2}\right)^2 + Du\frac{\partial^2 \phi}{\partial y^2} + \frac{1}{\Pr}\left(A_1 w + B_1 \theta\right).$$

(34)

$$\frac{\partial \psi}{\partial y}(q\frac{\phi}{z} + \frac{\partial \phi}{\partial z}) - \frac{\partial \psi}{\partial z}\frac{\partial \phi}{\partial y} = \frac{1}{Sc}\frac{\partial^2 \phi}{\partial y^2} + Sr\frac{\partial^2 \theta}{\partial y^2} - \gamma_1 \phi.$$

(37)

$$y = 0: \;\; \frac{\partial \psi}{\partial y} = z, \;\; \frac{\partial \psi}{\partial z} = f_w, \;\; N = -m\frac{\partial^2 \psi}{\partial y^2}, \;\; \theta = z^p, \;\; \phi = z^q$$

$$y \to \infty: \;\; \frac{\partial \psi}{\partial y} \to 0, \;\; N = 0, \;\; T \to T_\infty, \;\; C \to C_\infty$$

(38)

Lie Group Transformation

In order to transform the nonlinear partial differential equations (PDEs) governing the flow problem to nonlinear ordinary differential equations (ODEs), a simplified form of Lie group known as scaling group of transformations is used to obtain similarity variables and then to transform the partial differential equations (PDEs) of fluid flow to ordinary differential equations (ODEs).

Introducing Lie group scaling transformations Γ (Mukhopadhyay *et al.,* 2005, Uddin *et al*., 2015)

$$\Gamma: z^* = ze^{\varepsilon\alpha_1}, \;\; y^* = ye^{\varepsilon\alpha_2}, \;\; \psi^* = \psi e^{\varepsilon\alpha_3}, \;\; \theta^* = \theta e^{\varepsilon\alpha_4}$$

$$\phi^* = \phi e^{\varepsilon\alpha_5}, \;\; N^* = Ne^{\varepsilon\alpha_6}, \;\; w^* = we^{\varepsilon\alpha_7}, \;\; v^* = ve^{\varepsilon\alpha_8},$$

(39)

where α_i (i=1, 2…,8) are transformation parameters which are arbitrary real numbers not all zero simultaneously and ε is a small parameter of the group transformation.

Eqn. (3.112) is regarded as a point transformation which transforms coordinates

$(z, y, \psi, \theta, \phi, N, w, v))$ to the coordinates $(z*, y*, \psi*, \theta*, \phi*, N*, w*, v*)$.

Using Eq. (39) on (32-38) yields the following equations:

$$e^{\varepsilon(\alpha_1+2\alpha_2-2\alpha_3)}\left(\frac{\partial\psi^*}{\partial y^*}\frac{\partial^2\psi^*}{\partial z^*\partial y}-\frac{\partial\psi^*}{\partial z^*}\frac{\partial^2\psi^*}{\partial y^{*2}}\right)=(1+K)e^{\varepsilon(3\alpha_2-\alpha_3)}\frac{\partial^3\psi^*}{\partial y^{*3}}+Ke^{\varepsilon(\alpha_2-\alpha_6)}\frac{\partial N^*}{\partial y^*}+Gr\theta^* e^{-\varepsilon\alpha_4}+Gc\phi^* e^{-\varepsilon}$$

$$-(M+Da)e^{\varepsilon(\alpha_2-\alpha_3)}\frac{\partial\psi^*}{\partial y^*}-Fs(e^{\varepsilon(2\alpha_2-2\alpha_3)}\left(\frac{\partial\psi^*}{\partial y^*}\right)^2$$

$$e^{\varepsilon(\alpha_1+\alpha_2-\alpha_3-\alpha_6)}(\frac{\partial\psi^*}{\partial y^*}\frac{\partial N^*}{\partial z^*}-\frac{\partial\psi^*}{\partial z^*}\frac{\partial N^*}{\partial y^*})=\lambda e^{\varepsilon(2\alpha_2-\alpha_6)}\frac{\partial^2 N^*}{\partial y^{*2}}-I(2N^* e^{-\varepsilon\alpha_6}+e^{\varepsilon(2\alpha_2-\alpha_3)}\frac{\partial^2\psi^*}{\partial y^{*2}}.$$

$$e^{\varepsilon(\alpha_1+\alpha_2-\alpha_3-\alpha_4)}\left(\frac{\partial\psi^*}{\partial y^*}n\frac{\theta^*}{z^*}+\frac{\partial\psi^*}{\partial y^*}\frac{\partial\theta^*}{\partial z^*}-\frac{\partial\psi^*}{\partial z^*}\frac{\partial\theta^*}{\partial y^*}\right)=\frac{1}{Pr}\left(1+\frac{4}{3}R\right)e^{\varepsilon(2\alpha_2-\alpha_4)}\frac{\partial^2\theta^*}{\partial y^{*2}}+Ec(1+K)e^{\varepsilon(4\alpha_2-2\alpha_3)}\left(\frac{\partial^2\psi^*}{\partial y^{*2}}\right)^2$$

$$+Due^{\varepsilon(2\alpha_2-\alpha_5)}\frac{\partial^2\phi^*}{\partial y^{*2}}+\frac{1}{Pr}(A_1 e^{\varepsilon(\alpha_2-\alpha_3)}\frac{\partial\psi^*}{\partial y^*}+B_1\theta^* e^{-\varepsilon\alpha_4}).$$

$$e^{\varepsilon(\alpha_1+\alpha_2-\alpha_3-\alpha_5)}(q\frac{\phi^*}{z^*}\frac{\partial\psi^*}{\partial y^*}+\frac{\partial\psi^*}{\partial y^*}\frac{\partial\phi^*}{\partial z^*}-\frac{\partial\psi^*}{\partial z^*}\frac{\partial\phi^*}{\partial y^*})=\frac{1}{Sc}e^{\varepsilon(2\alpha_2-\alpha_5)}\frac{\partial^2\phi^*}{\partial y^{2*}}+Sre^{\varepsilon(2\alpha_2-\alpha_4)}\frac{\partial^2\theta^*}{\partial y^{2*}}$$

$$-\gamma_1 e^{-\varepsilon\alpha_5}\phi^*$$

(43)   The above system is invariant under the group transformation and the following relation exists among the parameters:

$$\alpha_1+2\alpha_2-2\alpha_3=3\alpha_2-\alpha_3=\alpha_2-\alpha_6=-\alpha_4=-\alpha_5=\alpha_2-\alpha_3=2\alpha_2-2\alpha_3 \qquad (44)$$

$$\alpha_1+\alpha_2-\alpha_3-\alpha_6=2\alpha_2-\alpha_6=-\alpha_6=2\alpha_2-\alpha_3$$

(45)

$$\alpha_1+\alpha_2-\alpha_3-\alpha_4=2\alpha_2-\alpha_4=4\alpha_2-2\alpha_3=2\alpha_2-\alpha_5=-\alpha_4$$

(46)

$$\alpha_1+\alpha_2-\alpha_3-\alpha_5=2\alpha_2-\alpha_5=2\alpha_2-\alpha_4=-\alpha_5.$$

(47)

The above system yields:

$$\alpha_1=\alpha_3=\alpha_4=\alpha_5=\alpha_6=\alpha_7.\,\alpha_2=\alpha_8=0,\ \alpha_3=\frac{1}{2}\alpha_1.$$

(48)

Thus the set of transformations Γ reduces to one parameter group of transformation as:

$$z^*=ze^{\varepsilon\alpha_1},\quad y^*=y,\ \psi^*=\psi e^{\varepsilon\alpha_1},\ \theta^*=\theta e^{\varepsilon\alpha_1}$$

$$\phi^*=\phi e^{\varepsilon\alpha_1},\quad N^*=Ne^{\varepsilon\alpha_1},\ w^*=we^{\varepsilon\alpha_1},\ v^*=v.$$

(49)

Condition for absolute invariance: The system of eqns. (3.114) -(3.117) as well as those for the boundary will be absolute invariant if the structure of the eqns. remains unchanged before and after the transformations.

In consequence, the first absolute invariant η which is a function of the independent variables is taken as

$$\eta=y^* z^{*a},\ \eta=y^* z^a e^{\varepsilon\alpha_1 a}$$

(50)

Thus setting $a=0$ (since α_1 cannot be 0) to get an absolute invariant

$$\eta = y^{*}.$$

(51)

Similarly, the second absolute invariant $f(\eta)$ which involves the dependent variable ψ^{*} is

$$f(\eta) = z^{*b}\psi^{*} = z^{b}e^{\varepsilon\alpha_{1}b}\psi e^{\varepsilon\alpha_{1}}, \ \psi z^{b}e^{\varepsilon\alpha_{1}(b+1)}$$

(52)

setting $b = -1$ (since α_{1} cannot be 0) in the preceding equation as to get

$$f(\eta) = \psi^{*}z^{*-1}$$

(53)

Following similar procedural steps,

$$g(\eta) = z^{*c}N^{*} \ \text{i.e.,} \ z^{c}e^{\varepsilon\alpha_{1}c}Ne^{\alpha_{1}c} = z^{c}Ne^{\varepsilon\alpha_{1}(c+1)}$$

(54)

$$g(\eta) = z^{*-1}N^{*}.$$

(55)

Similarly, the other variables are gotten in the same manner as

$$\theta(\eta) = z^{*d}\theta^{*} = \theta^{*}z^{*-1}$$

(56)

$$\phi(\eta) = z^{*e}\phi^{*} = \phi^{*}z^{*-1}$$

(57)

Eqns. yield the following similarity variables

$$\eta = y^{*}, \ \psi^{*} = z^{*}f(\eta), \ N^{*} = z^{*}g(\eta), \ \theta^{*} = z^{*}\theta(\eta), \ \phi^{*} = z^{*}\phi(\eta)$$

(58)

Applying Eq. (58) on eqns. (40-43) to get following nonlinear ordinary differential equations:

$$(1+K)f''' + ff'' - (Fs+1)f'^{2} + Kg' + Gr\theta + Gc\phi - (Da+M)f' = 0.$$

(59)

$$\lambda g'' + fg' - f'g - I(2g + f'') = 0.$$

(60)

$$(1+\frac{4}{3}R)\theta'' + \Pr Ec(1+K)f''^{2} + \Pr Du\phi'' - \Pr \zeta\theta f' + \Pr f\theta' + (A_{1}f' + B_{1}\theta) = 0.$$

(61)

$$\phi'' + ScSr\theta'' + Scf\phi' - Sc\delta\phi f' - Sc\gamma_{1}\phi = 0.$$

(62)

The corresponding boundary conditions are

$$\eta = 0: f' = 1, f = f_{w}, \ g = -mf'', \ \theta = 1, \ \phi = 1$$
$$\eta \to \infty: f' \to 0, \ g = 0, \ \theta \to 0, \ \phi \to 0$$

(63)

Where prime denotes the differentiation with respect to η, $\zeta = p + 1$ and $\delta = q + 1$.

Quantities of engineering interest

The quantities of main physical interest are the skin friction coefficient, wall couple stress, the Nusselt number (rate of heat transfer) and the Sherwood number (mass transfer rate). These are respectively defined as:

$$C_{f\bar{z}} = \frac{\tau_w}{\rho w_w^2}, \text{ where, } \tau_w = \left[\left(\mu+\kappa\right)\frac{\partial \overline{w}}{\partial \overline{y}} + \kappa \overline{N}\right]_{\overline{y}=0}$$

(64)

$$M_{\bar{z}} = \left(\gamma \frac{\partial \overline{N}}{\partial \overline{y}}\right)_{\overline{y}=0}$$

(65)

$$Nu_{\bar{z}} = \frac{\overline{z} q_w}{\text{k}(T_w - T_\infty)}, \text{ where, } q_w = -k\left(\frac{\partial T}{\partial \overline{y}}\right)_{\overline{y}=0}$$

(66)

$$Sh_{\bar{z}} = \frac{\overline{z} q_m}{\text{D}_m(\text{C}_w - C_\infty)}, \text{ where, } q_m = -D_m\left(\frac{\partial C}{\partial \overline{y}}\right)_{\overline{y}=0}$$

(67)

Numerical Simulation

The set of equations (59) -(62) and the boundary conditions (63) have been solved numerically using a shooting algorithm with a Runge Kutta Fehlberg fourth fifth integration scheme. A systematic guessing of $f''(0), \theta'(0), \phi'(0)$ and $g'(0)$ have been accessed until upstream boundary conditions are gotten asymptotically. Use has been made of the step-size $\Delta\eta = 10^{-3}$. Based on this technique, a finite value η_∞ has been adopted in place of $\eta \to \infty$ which depends on the parametric values. Also the computations are carried out by a program coded in a symbolic and computational computer language, Maple-2016. From the process of numerical computations, the skin friction co-efficient, Nusselt number, Sherwood number and wall couple stress are all sorted out and their numerical values are presented in a tabular form.

RESULTS AND DISCUSSION.

In order to validate the numerical results obtained, comparison is made with those reported by Grubka & Bubba (1985), Ali (1994), Ishak (2008), Chen (1988), Srinivas *et al* (2013) and Qasim *et al*. (2013).

TABLE 1. Comparison of $-\theta(0)$ for $m = 0.5, K = 0$ and for various values of Pr with previously published data.

Pr	Grubka & Bubba	Ali	Ishak	Chen	Srinivas *et al.*	Qasim *et al.*	Present
0.72	0.4631	0.4617	0.4631	0.46315	0.46314	0.46360	0.46325
1.0	0.5820	0.5801	0.5820	0.58199	0.58197	0.58202	0.58198
3.0	1.1652	1.1599	1.16523	1.16523	1.16525	1.16525	1.16525
7.0	▬	▬	▬	▬	▬	1.89542	1.89540
10.0	2.3080	2.2960	2.3080	2.30796	2.30800	2.30800	2.30800
100	7.7657		7.7657	7.76565	7.76565	7.58261	7.76564

TABLE 2. EFFTECTS OF SKIN FRICTION, NUSSELT NUMBER, SHERWOOD NUMBER AND WALL COUPLE STRESS FOR VARIOUS VALUES OF Pr, R, A, B, K &M

Pr	R	A	B	K	M	$-f''(0)$	$-\theta'(0)$	$-\phi'(0)$	$-g'(0)$
0.72	0.1	0.1	0.1	1.0	0.1	0.80264	0.52333	0.45141	0.39371

12

1.0	0.1	0.1	0.1	1.0	0.1	0.81038	0.67439	0.44060	0.39671
3.0	0.1	0.1	0.1	1.0	0.1	0.83154	1.37718	0.39364	0.40646
7.0	0.1	0.1	0.1	1.0	0.1	0.84247	2.29225	0.33419	0.41282
1.0	1.0	0.1	0.1	1.0	0.1	0.78425	0.44983	0.43394	0.39098
1.0	3.0	0.1	0.1	1.0	0.1	0.76975	0.28993	0.44943	0.38708
1.0	4.0	0.1	0.1	1.0	0.1	0.76604	0.25493	0.45315	0.38619
1.0	5.0	0.1	0.1	1.0	0.1	0.76339	0.23089	0.45576	0.38558
1.0	0.2	0.5	0.1	1.0	0.1	0.78198	0.36667	0.43925	0.38980
1.0	0.2	1.0	0.1	1.0	0.1	0.76314	0.01636	0.46540	0.38290
1.0	0.2	1.5	0.1	1.0	0.1	0.74372	0.34573	0.49185	0.37562
1.0	0.2	0.1	0.3	1.0	0.1	0.78694	0.47477	0.43132	0.39168
1.0	0.2	0.1	0.5	1.0	0.1	0.76875	0.22012	0.45190	0.38558
1.0	0.2	0.1	0.7	1.0	0.1	0.73293	0.24053	0.48805	0.37328
1.0	0.2	0.1	1.0	1.0	0.1	0.64216	1.51231	0.57618	0.33813
1.0	0.2	0.1	0.1	0.5	0.1	0.85947	0.63978	0.41089	0.43518
1.0	0.2	0.1	0.1	2.0	0.1	0.70866	0.63311	0.43192	0.34171
1.0	0.2	0.1	0.1	3.0	0.1	0.64800	0.62815	0.44276	0.30660
1.0	0.2	0.1	0.1	5.0	0.1	0.56615	0.61804	0.45942	0.26132
1.0	0.2	0.1	0.1	1.0	0.3	0.86513	0.61014	0.40947	0.43595
1.0	0.2	0.1	0.1	1.0	0.6	0.94883	0.30079	0.41358	0.48969
1.0	0.2	0.1	0.1	1.0	1.0	1.02996	0.22750	0.44542	0.55106

TABLE 3. EFFTECTS OF SKIN FRICTION, NUSSELT NUMBER, SHERWOOD NUMBER   AND WALL COUPLE STRESS FOR VARIOUS VALUES OF Gr, Gc, Sc, Du, Sr & γ

Gr	Gc	Sc	Du	Sr	γ	$-f''(0)$	$-\theta'(0)$	$-\phi'(0)$	$-g'(0)$
0.9	0.5	0.22	0.1	2.0	0.1	0.85450	1.09769	0.23845	0.45018
1.3	0.5	0.22	0.1	2.0	0.1	0.73718	1.12754	0.24299	0.36664
1.5	0.5	0.22	0.1	2.0	0.1	0.67972	1.14114	0.24522	0.32512
0.5	0.9	0.22	0.1	2.0	0.1	0.79988	1.12668	0.25516	0.42568
0.5	1.3	0.22	0.1	2.0	0.1	0.63192	1.17651	0.26571	0.31604
0.5	1.5	0.22	0.1	2.0	0.1	0.55033	1.19789	0.27201	0.26106
0.5	0.5	0.22	0.1	2.0	0.1	0.97581	1.06349	0.23376	0.53455
0.5	0.5	0.68	0.1	2.0	0.1	0.99607	1.04488	0.29779	0.53874
0.5	0.5	0.72	0.1	2.0	0.1	0.99885	1.04247	0.30445	0.53944
0.5	0.5	0.22	0.5	2.0	0.1	0.97269	1.04978	0.23926	0.53386
0.5	0.5	0.22	1.0	2.0	0.1	0.96860	1.03432	0.24503	0.53288
0.5	0.5	0.22	1.2	2.0	0.1	0.96691	1.02917	0.24676	0.53244
0.5	0.5	0.22	0.1	1.0	0.1	0.99035	1.04443	0.40228	0.54030
0.5	0.5	0.22	0.1	2.0	0.1	0.97581	1.06349	0.23376	0.53455
0.5	0.5	0.22	0.1	3.0	0.1	0.96120	1.08248	0.05932	0.52858
0.5	0.5	0.22	0.1	2.0	0.3	0.98500	1.05440	0.29340	0.53693
0.5	0.5	0.22	0.1	2.0	0.5	0.99105	1.04646	0.34664	0.53902
0.5	0.5	0.22	0.1	2.0	0.7	0.99701	1.03942	0.39502	0.54088

Steady MHD micropolar fluid flow past a vertical stretching permeable surface embedded in a porous medium is studied in this work. The effects of various governing flow parameters namely;

13

Magnetic field parameter M, material parameter K (Eringen parameter), diffusion-thermo (Dufour) Du, thermo-diffusion (Soret) Sr, thermal buoyancy parameter (Grashof number) Gr, solutal buoyancy parameter Gc, space dependent heat source/sink parameter, A, temperature dependent heat source/sink parameter B and suction/injection parameter fw have been considered on the dimensionless velocity, temperature, concentration and microrotation profiles of the flow.

Computation of the rate of heat transfer were carried out and compared with previous published works. The comparison shows good agreement of this work with the previous published results as presented in table 1.

Table 2 presents the skin friction coefficient, Nusselt number, Sherwood number and wall couple stress for various values of flow parameters Pr, M, R, A, B and K. From the table, it is seen that the skin friction coefficient numerically increases with increase in the Prandtl number Pr and Magnetic parameter M. On the other hand, the skin friction reduces numerically with increase in radiation parameter R, space and temperature dependent heat source/sink A & B and material parameter K. Thus the parameters K can be used to reduce the skin friction on the boundary. This result is in good agreement Kumar (2009).

From Table 2, it is evident that the heat transfer rate increases with increase in Prandtl number while it decreases with increase in R, K and M respectively. Similarly, from the table, it was observed that the rate of mass transfer (Sherwood number) decreases with increase in Pr while it increases with R, K and M. The wall couple stress $-g'(\theta)$ numerically increases with Pr and M while it falls numerically with increase in R, A, B and K.

Table 3 illustrates the effects of thermal Grashof number,Gr, Solutal Grashof number,Gc Schmidt, Dufour number Soret number and chemical reaction on the skin friction coefficient, $-f''(\theta)$, rate of heat transfer $-\theta'(0)$, rate of mass transfer $-\phi^1(0)$ and wall couple stress $-g'(\theta)$.From the table it is evident that the skin friction coefficient decreases with increase in $Gr, Gc, Du, and\ Sr$ while it increase with the increase in Schmidt number Sc and chemical reaction γ respectively. It was observed as well that both Gr and Gc tend to increase the rate of heat and mass transfer while Dufour and Soret numbers tend to reduce heat transfer rate. In the like manner, Dufour number Du tends to increase $-\phi'(\theta)$ while Soret number Sr reduces it.

Fig.2 (a-d) shows the effect of magnetic parameter on the velocity, temperature, concentration and microrotation profiles. It was observed that the magnetic parameter M reduces the velocity distribution. This indicates that the fluid velocity can be reduced by increasing in the magnetic field. This reduction of velocity is attributed to the Lorentz force, a resistive force, causes a reduction along the main direction of flow. This result is in good agreement with Kumar (2009) and Mishra *et al.,* (2016).The three other profiles exhibit an opposite trend.

Fig.3 (a-d) depicts the effects of the material parameter $K\left(\frac{\kappa}{\mu}\right)$ the flow profiles. It is evident from Fig 3a that the velocity increases with increase in K. Similarly, temperature profiles also increase with the increase in parameter K as shown in fig 3b. Hence material parameter K enhances the increase in the thermal boundary layer.

The effects of material parameter K on the concentration profile (Fig.3c) shows that the concentration decreases with increase in K. The influence of K on microrotation profile is shown in Fig 3d. It shows that microrotation decrease greatly with increase in K near the wall. This implies that the more concentration of the particles reduce the microrotation near the boundary.

Fig. 4 depicts the effects of thermo-diffusion (Soret) on the concentration profile. It is clear from the figure that increase in Soret number increases the concentration distribution.

Fig. 5 (a-b) illustrates the velocity and temperature profiles with diffusion-thermo (Dufour). The velocity boundary layer decreases with increase in Dufour number while thermal boundary layer increases with Dufour number.

Fig. 6 (a-d) demonstrates the effects of space dependent heat source/sink parameter A. Fig. 6(a-b) reveals that both velocity and temperature profiles are enhanced with the increase in A. The influence of A on microrotation distribution is of dual character as shown in Fig. 6d. It decreases near the boundary while it increases away from the boundary. In like manner Fig. 7(a-b) illustrates the influence of temperature dependent heat source/sink on the velocity and temperature profiles. It is seen from the figure that both velocity and temperature profiles increase with the increase in the temperature dependent heat/source sink parameter, B, on the contrary the increase in B reduces concentration distribution as shown in Fig 7c while parameter B has a dual influence on microrotation profile as shown in Fig. 7d.

Fig.8 (a-d) depicts the effect of the wall mass transfer (suction/injection) fw on the velocity, temperature, concentration and microrotation profiles respectively. It is clearly seen that imposition of wall suction ($fw > 0$) decreases the velocity, temperature, concentration as well as the microrotation profiles and their boundary layer thicknesses, the opposite is seen with fluid wall injection ($fw < 0$), the flow profiles increase with injection.

From Fig 9a it is shown that the velocity profile decreases with the increase in the Prandtl number. Similarly Fig 9b exhibits the influence of the Prandtl number Pr on the temperature profile. It is evident that temperature distribution decreases with increase in the Prandtl number. Thus temperature in the boundary layer drops very fast as Pr increases because the thermal boundary layer thickness decreases with increase in the Prandtl number.

Fig 10 (a-d) reveals the effects of thermal buoyancy parameter (Grashof number) Gr on the flow profiles. It is observed that (Fig 10a) the increase in Gr enhances the velocity distribution. On the contrary, the temperature and concentration profiles decrease as Gr increases as shown in Fig. 10 (b-c). The microrotation profile Fig. (10d) decreases near the wall with increase in Gr while it increases slightly away from the boundary.

In a similar manner the effect of increasing the Solutal Grashof number Gc is to increases the velocity profile and retards the temperature and concentration distribution as shown in Fig 11.

CONCLUSIONS

The present study numerically studies the flow, heat and mass transfer of MHD micropolar fluid flow past a vertically stretching permeable mate in Darcy-Forchheimer porous medium. The influence of various governing flow parameters such as the magnetic parameter M, material parameter K, thermal and solutal buoyancy parameters Gr & Gc, Soret and Dufour number (Sr and Du), space dependent and temperature dependent heat source/sink parameter (A & B) with suction/injection parameter, fw have be analyzed.

The governing PDEs were transformed into ODEs using Lie group scaling transformation and resulting coupled non-linear odes were numerically solved using Runge-Kutta Fehlberg fourth fifth integration scheme alongside the shooting method.

From this study, the following observations were made.
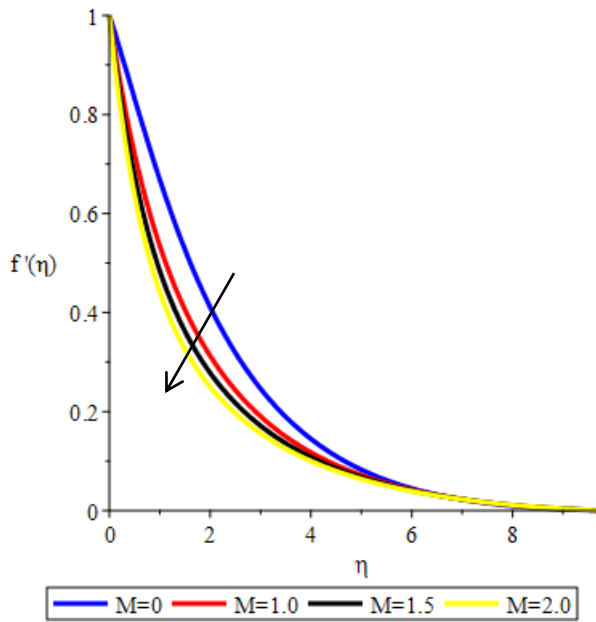
Fig.2a. Velocity profiles for various values of M (K=0.5, Gr=Gc=1.0, Ec=2, Fs=0.5=Du=Sr=0.5, $\zeta = \delta = 2$)
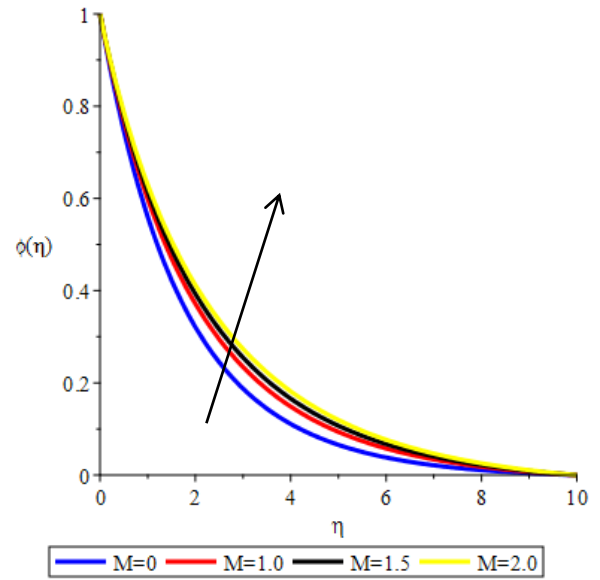
Fig.2c. Concentration profiles for various values of M (K=0.5, Gr=Gc=1.0, Ec=2, Fs=0.5 =Du=Sr=0.5, $\zeta = \delta = 2$)
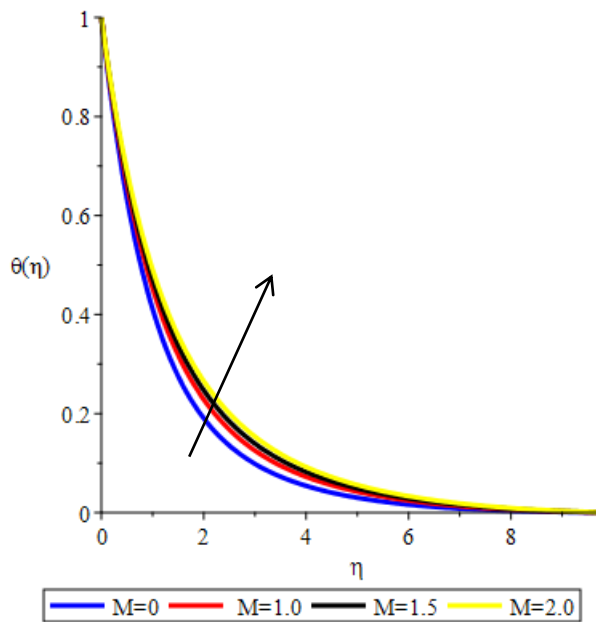
Fig.2b. Temperature profiles for various values of M (K=0.5, Gr=Gc=1.0, Ec=2, Fs= Du=Sr=0.5, $\zeta = \delta = 2$)
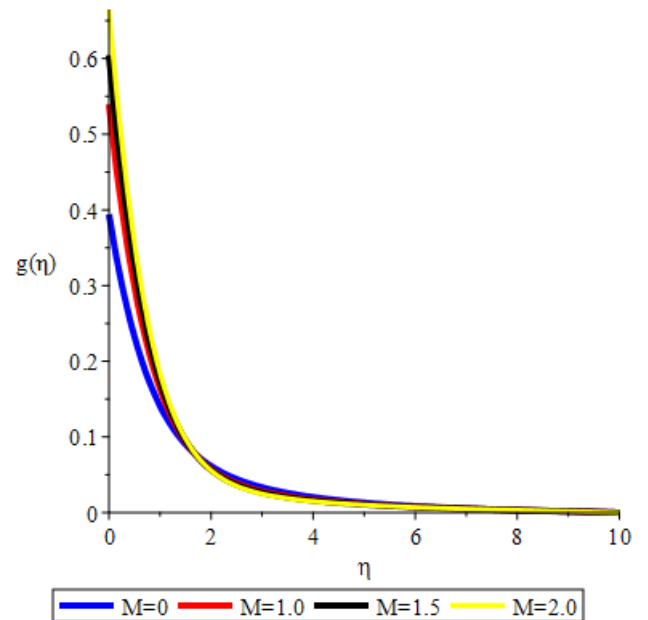
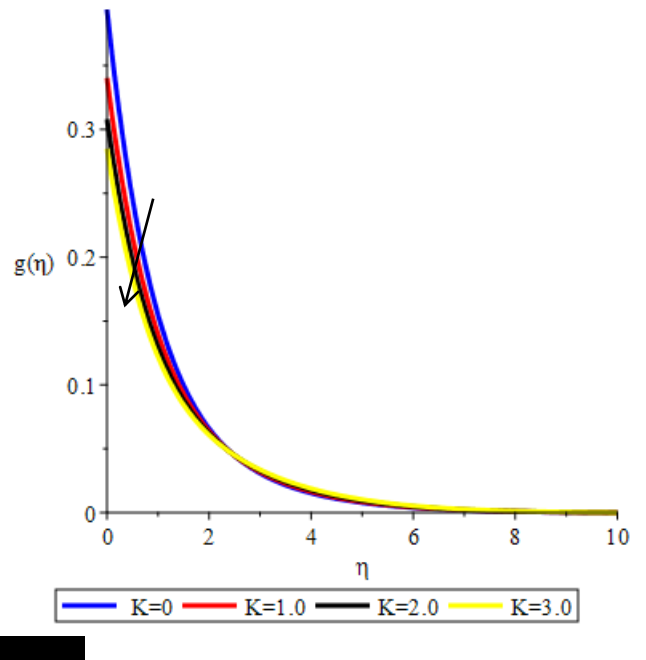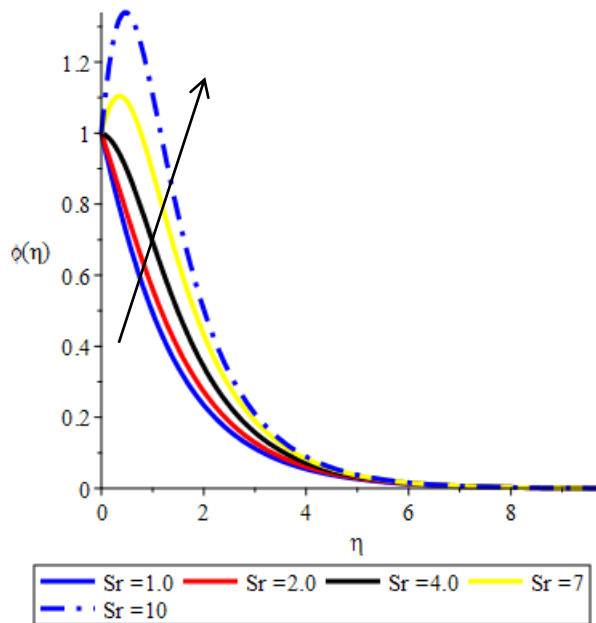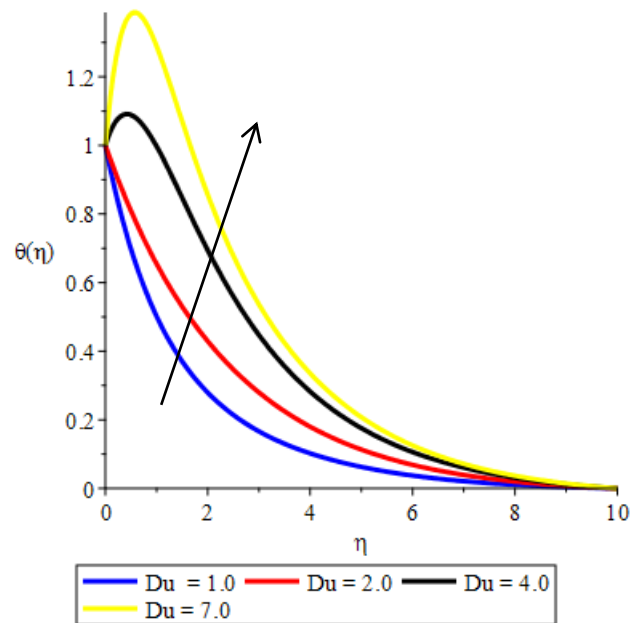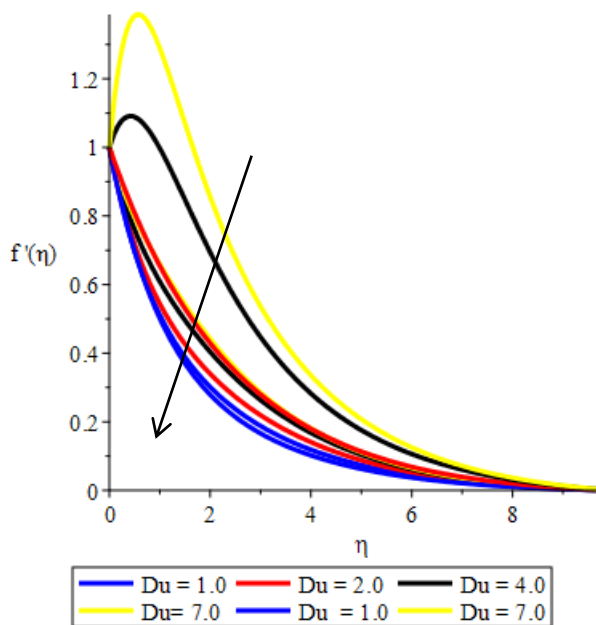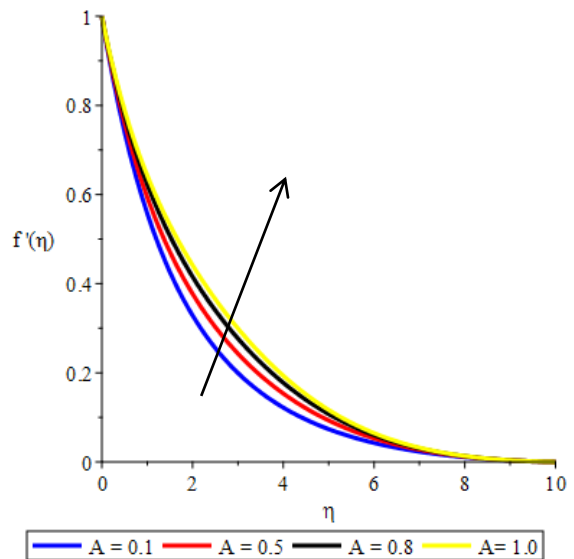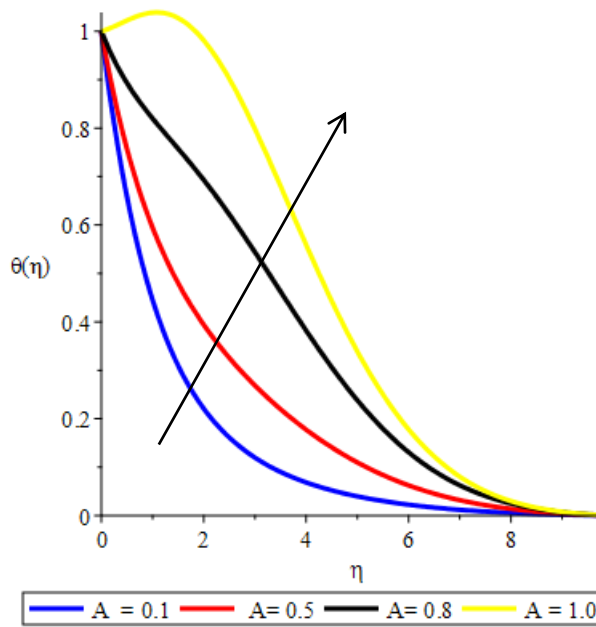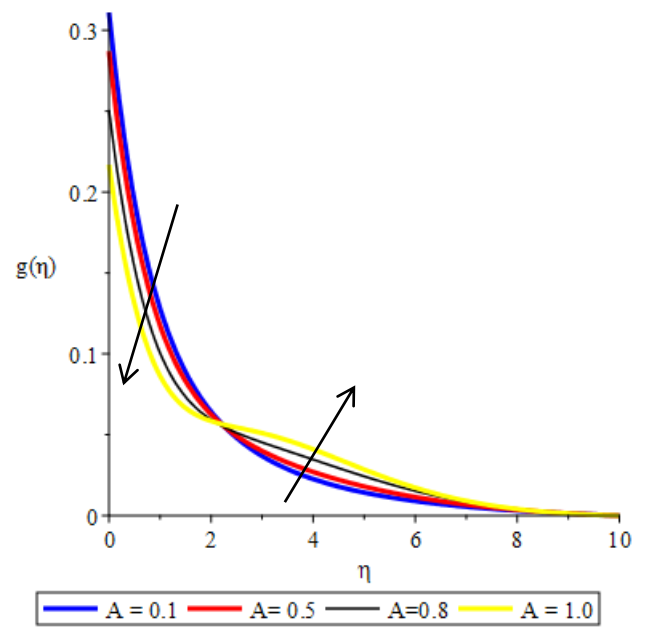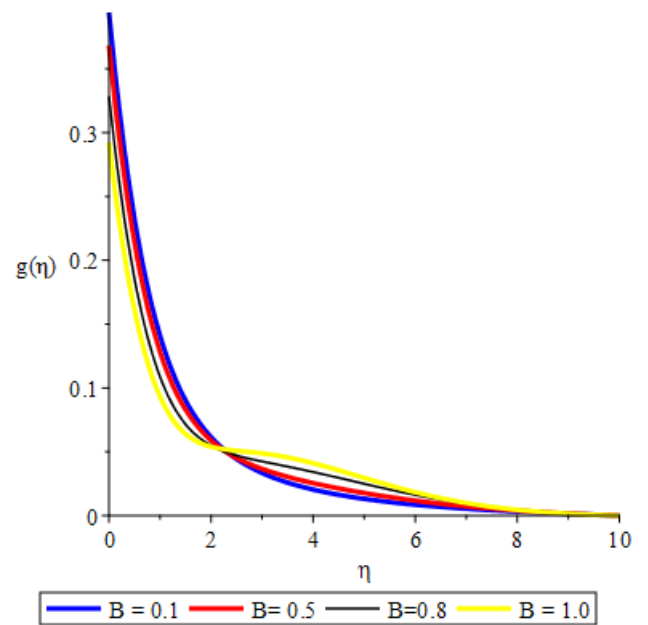**Fig.2d**. Microrotation profiles for various values of M (K=0.2, Gr=Gc=1.0, Ec=2, Fs=0.5= Du=Sr=0.5)
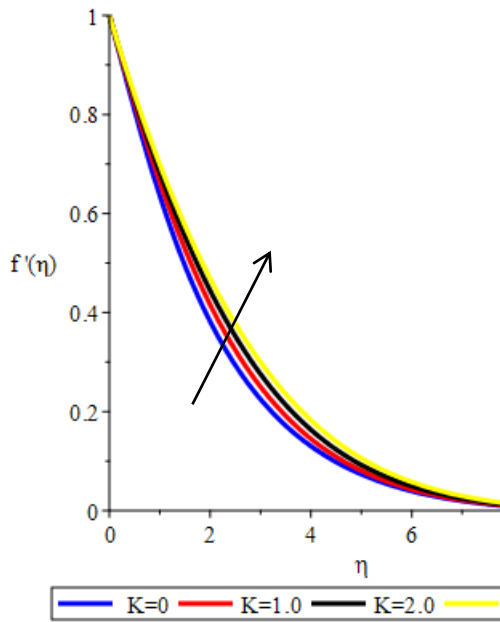
Fig.3a. Velocity profiles for various values of K(M=0.2, Gr=Gc=1.0, Ec=2.0, Fs=0.5=Du=Sr=0.5, $\zeta = \delta = 2$)
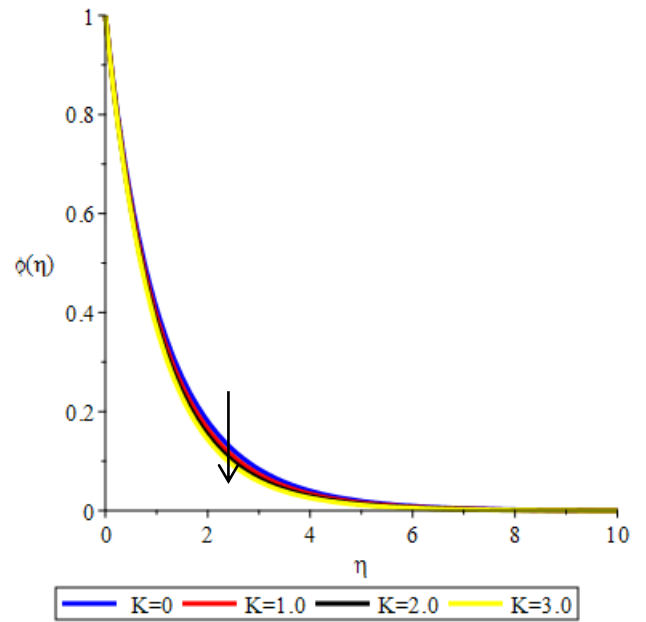
Fig.3c. Concentration profiles for various values of K(M=0.2, Gr=Gc=1.0, Ec=0.2, Fs=Du=Sr=0.5, $\zeta = \delta = 2$)
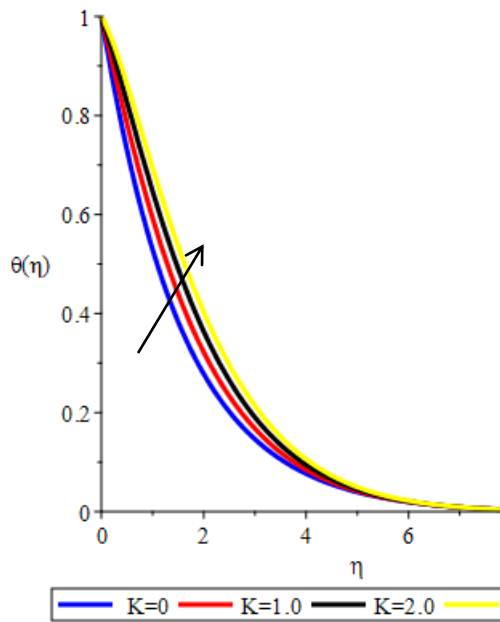
Fig.3b. Temperature profiles for various values of K (M=0.2, Gr=Gc=1.0, Ec=0.2, Fs=0.5. Du=0.5, Sr=0.5,$\zeta = \delta = 2$)

Fig.3d. Microrotation profiles for various values of K (M=0.2, Gr=Gc=1.0, Ec=0.2, Fs=0.5=Du=Sr=0.5, $\zeta = \delta = 2$)

17

Fig.4. Concentration profiles for various values of Sr (M=0.1, Gr=Gc=1.0, Ec=0.2, Fs=0.5, Du=0.5, $\zeta = \delta = 2$)

Fig.5b. Temperature profiles for various values of Du (M=0.1, Gr=Gc=5.0, Ec=0.2, Fs=Sr=0.5, $\zeta = \delta = 2$)

Fig.5a. Velocity profiles for various values of Du (M=0.1, Gr=Gc=1.0, Ec=0.2, Fs= Sr=0.5, $\zeta = \delta = 2$)

Fig.6a. Velocity profiles for various values of A (M==B=0.1, Gr=Gc=5.0, Ec=0.2, Fs= Sr=Du=0.5, $\zeta = \delta = 2$)

Fig.6b. Temperature profiles for various values of A (M=0.1,B=0.1, Gr=Gc=5.0, Ec=0.2, Fs=Sr= Du=0.5,$\zeta = \delta = 2$)

Fig.6d. Microrotation profiles for various values of A (M=0.1,B=0.1, Gr=Gc=5.0, Ec=0.2, Fs=, Du=0.1, $\zeta = \delta = 2$)
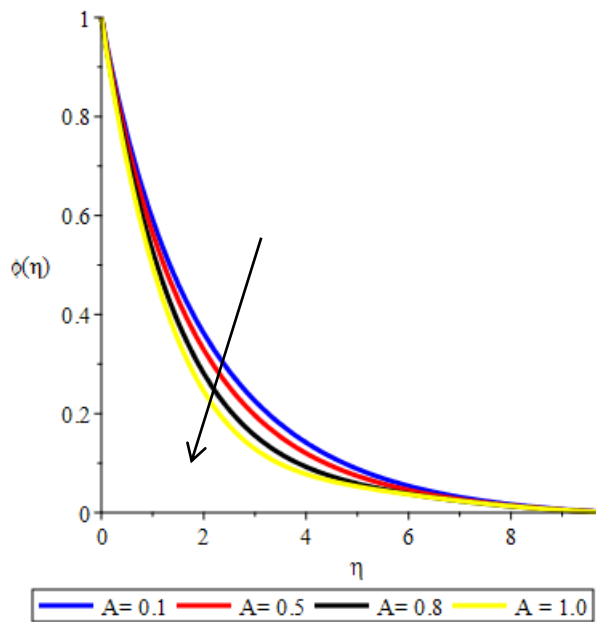
Fig6c. Concentration profiles for various values of A (M=0.1, Gr=Gc=5.0, Ec=0.2, Fs=Sr= Du=0.5, $\zeta = \delta = 2$)
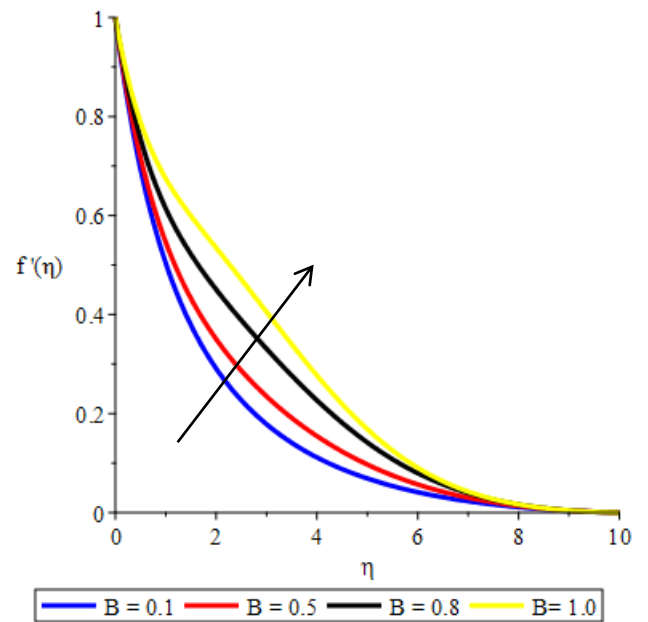
Fig.7a. Velocity profiles for various values of B (M=0.1,A=0.1 Gr=Gc=5.0, Ec=0.2, Fs=Sr=Du=0.5, $\zeta = \delta = 2$)
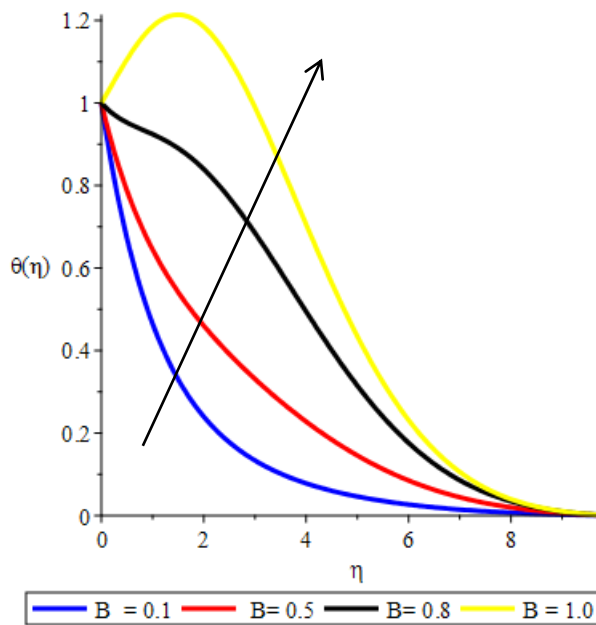
Fig.7b. Temperature profiles for various values of B (M=0.1, A=0.1,Gr=Gc=5.0, Ec=0.2, Fs=Sr= Du=0.5, $\zeta = \delta = 2$)

Fig.7d. Velocity profiles for various values of B (M=0.1, A=0.1,Gr=Gc=5.0, Ec=0.2, Fs=0.5=Sr=Du=0.5, $\zeta = \delta = 2$)
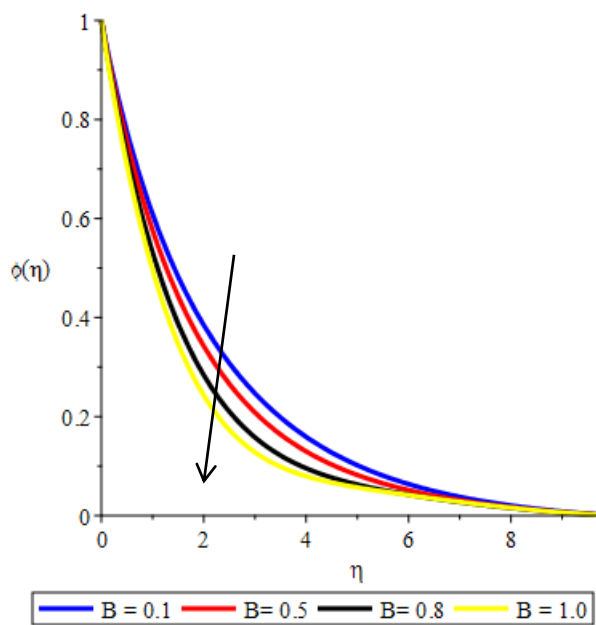
Fig.7c. Concentration profiles for various values of B (M=0.1, A=0.1,Gr=Gc=5.0, Ec=0.2, Fs=Sr= Du=0.5,$\zeta = \delta = 2, Pr = 0.72$)
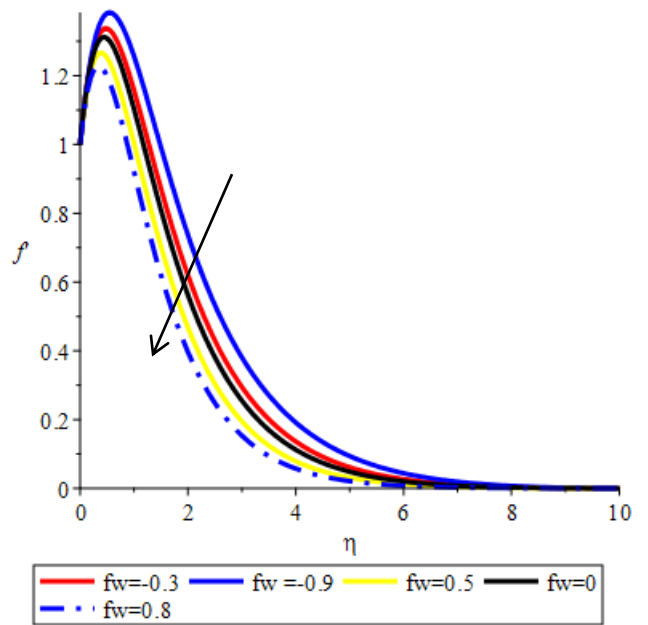
Fig.8a. Velocity profiles for various values of fw (Gr=Gc=5.0, Sr= Du =M=0.5, $\zeta = \delta = 2, Ec = 0.2$)
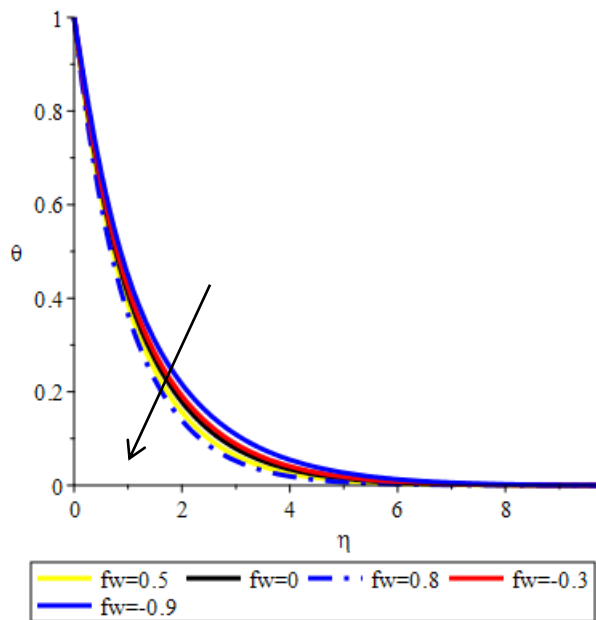
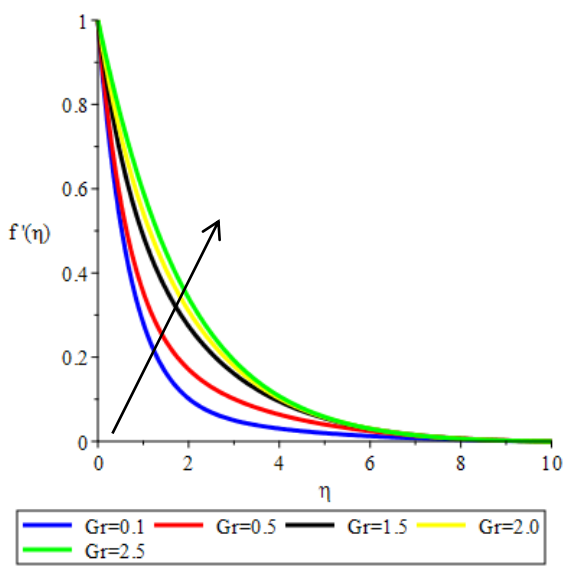**Fig.8b**. Temperature profiles for various values of fw (Gr=Gc=5.0, Sr= Du =M=0.5, $\zeta = \delta = 2, Ec = 0.2, Pr = 0.72$)
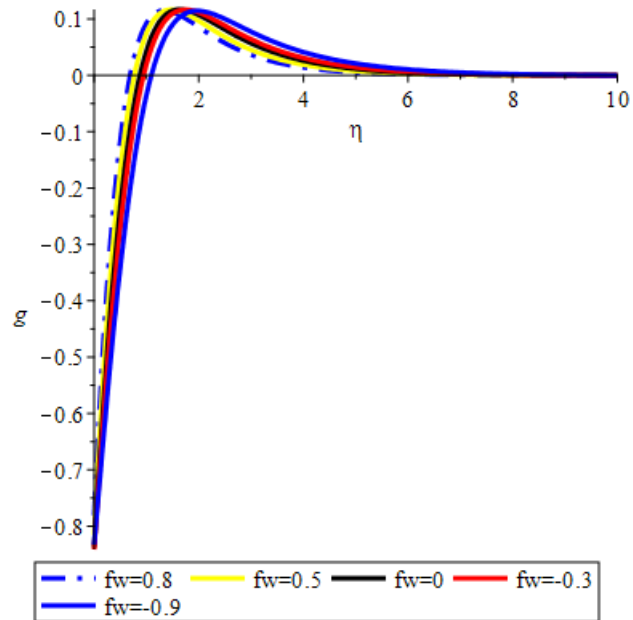
Fig.8d. Microrotation profiles for various values of fw (Gr=Gc=5.0, Sr= Du =M=0.5, $\zeta = \delta = 2, Ec = 0.2, Pr = 0.72$)
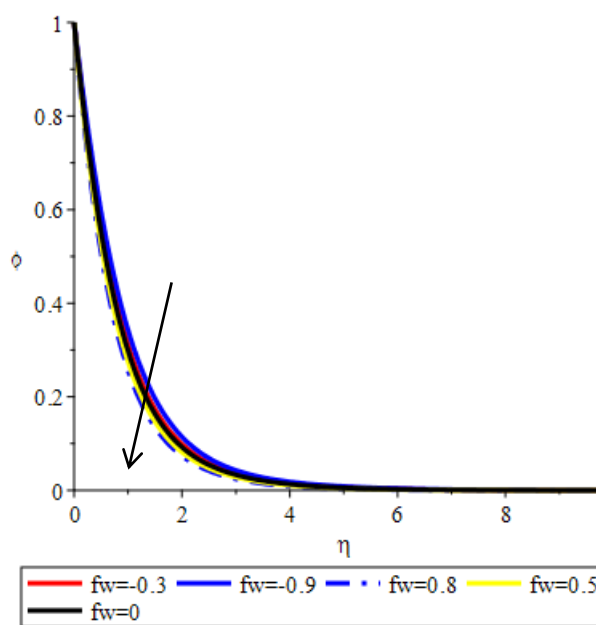
Fig.8c. Concentration profiles for various values of fw (Gr=Gc=5.0, Sr= Du =M=0.5, $\zeta = \delta = 2, Ec = 0.2, Pr = 0.72$)
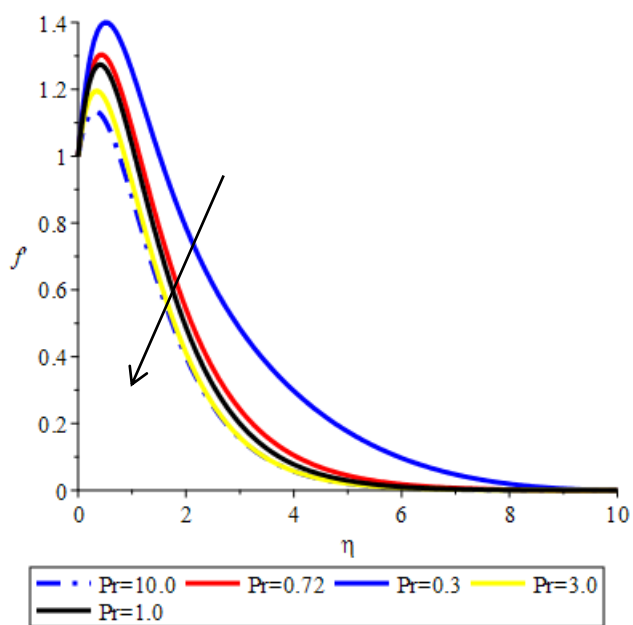
Fig.9a. Microrotation profiles for various values of Pr (Gr=Gc=5.0, Sr= Du =M=0.5, $\zeta = \delta = 2, Ec = 0.2$)

21
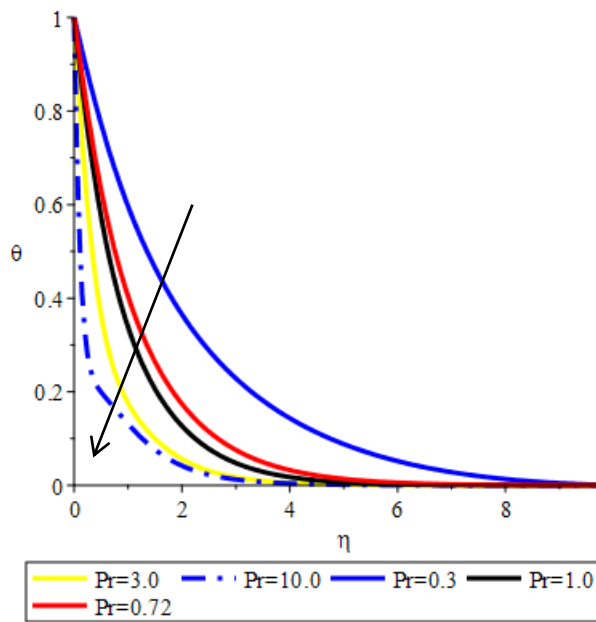
Fig.9b. Temperature profiles for various values of Pr (Gr=Gc=5.0, Sr= Du =M=0.5, $\zeta = \delta = 2, Ec = 0.2$).
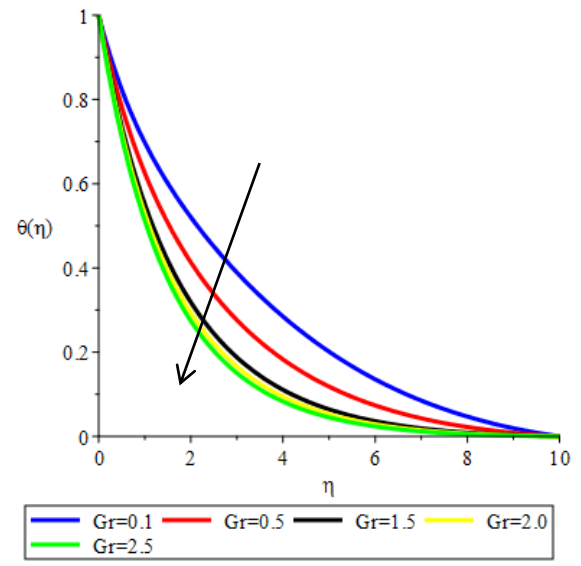
Fig.10b Temperature profiles for various values of Gr (Gc=0.1, M=0.2, Da=1.0, Sr= Du =Fs=0.5, $\zeta = \delta = 2, Ec = 0.2$).

Fig.10a Velocity profiles for various values of Gr (Gc=0.1, M=0.2, Da=1.0, Sr= Du =Fs=0.5, $\zeta = \delta = 2, Ec = 0.2$).
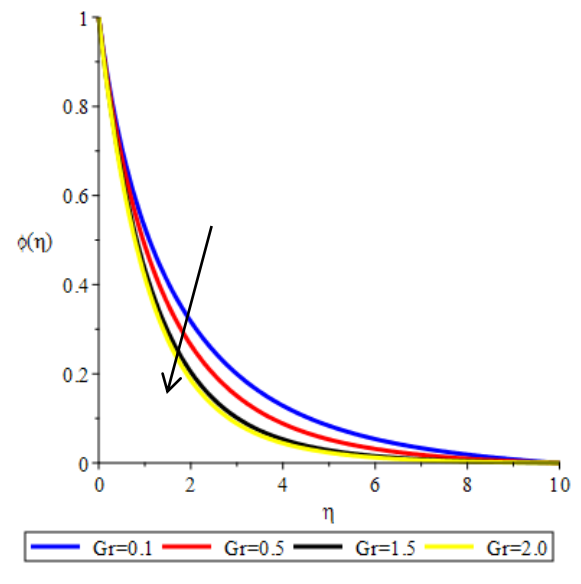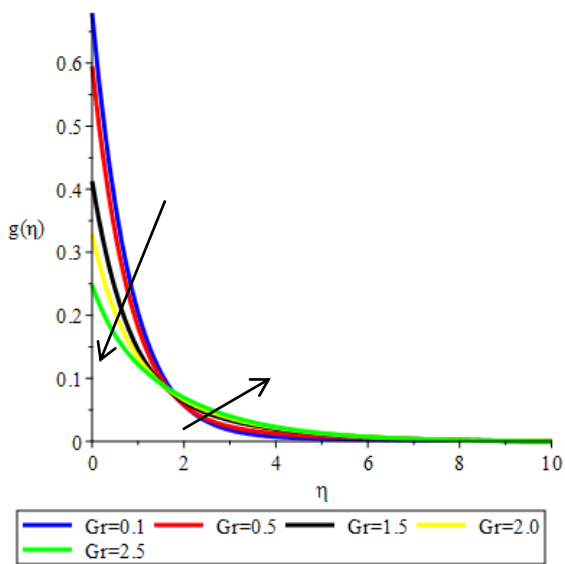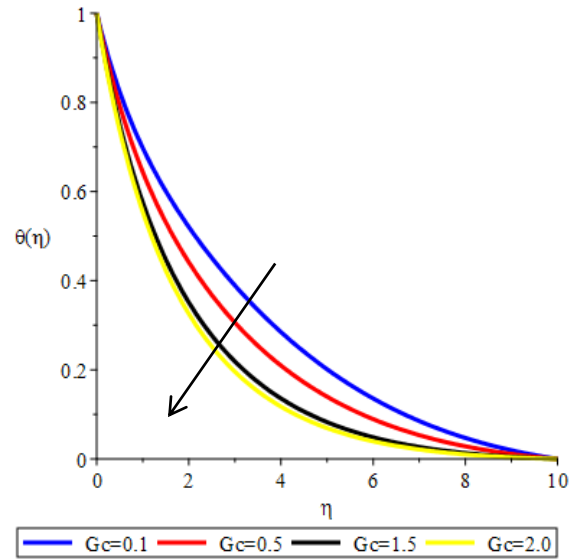

Fig.10c Concentration profiles for various values of Gr (Gr=0.1, M=0.2, Da=1.0, Sr= Du =Fs=0.5, $\zeta = \delta = 2, Ec = 0.2$).

Fig.10d Microrotation profiles for various values of Gr (Gc=0.1, M=0.2, Da=1.0, Sr= Du =Fs=0.5, $\zeta = \delta = 2, Ec = 0.2$).

Fig.11b Temperature profiles for various values of Gc (Gr=0.1,M=0.2,Da=1.0, Sr= Du =Fs=0.5, $\zeta = \delta = 2, Ec = 0.2$).
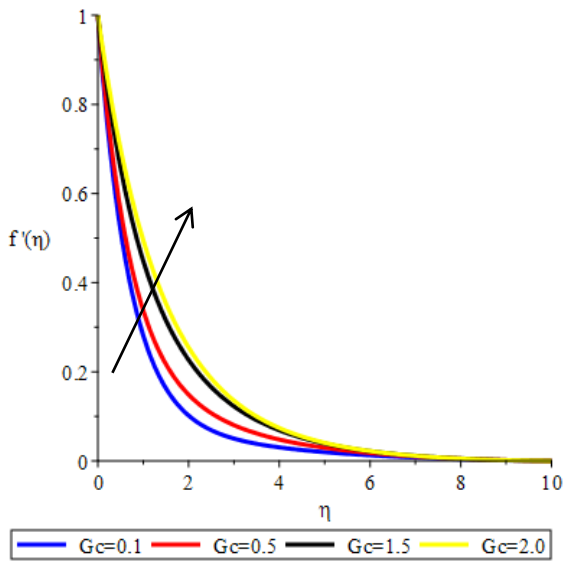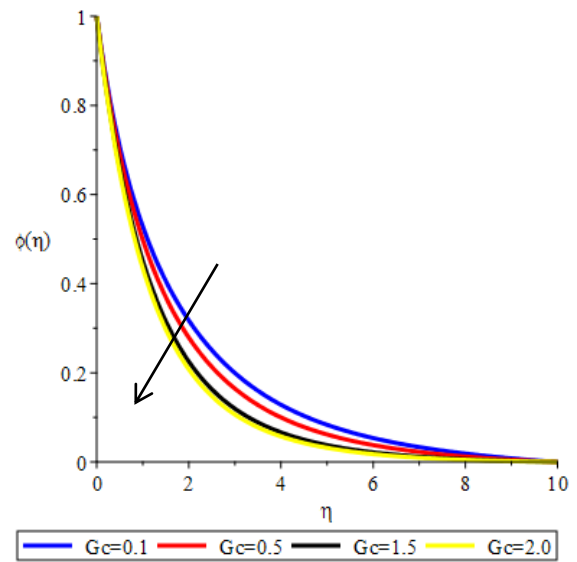

Fig.11a Velocity profiles for various values of Gc (Gr=0.1, M=0.2, Da=1.0, Sr= Du =Fs=0.5, $\zeta = \delta = 2, Ec = 0.2$).

Fig.11c Velocity profiles for various values of Gc (Gr=0.1, M=0.2, Da=1.0, Sr= Du =Fs=0.5, $\zeta = \delta = 2, Ec = 0.2$).
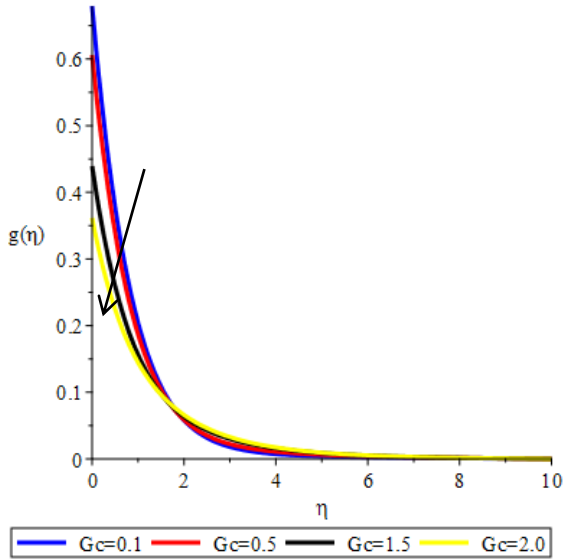
.

23

Fig.11d Microrotation profiles for various values of Gc (Gr=0.1, M=0.2, Da=1.0, Sr= Du =Fs=0.5, $\zeta = \delta = 2, Ec = 0.2$)
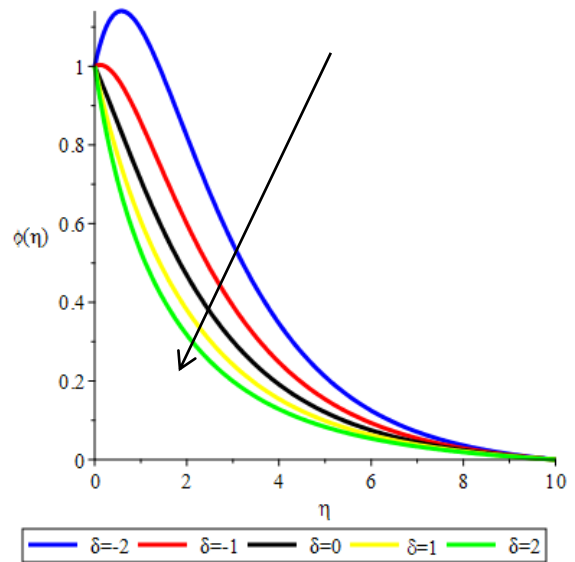

Fig.13 Concentration profiles for various values of δ (Gr=0.1, M=0.2, Da=1.0, Sr= Du =Fs=0.5, $Pr = 0.72, Sc = 0.22, \zeta = 2, Ec = 0.2$).
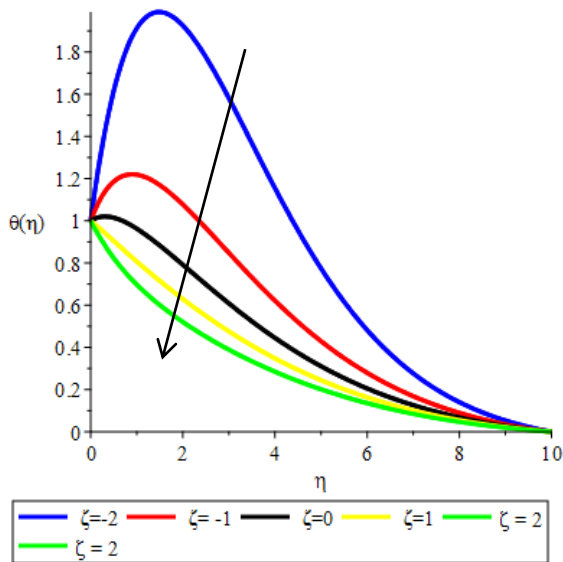

Fig.12 Temperature profiles for various values of ζ (Gr=0.1, M=0.2, Da=1.0, Sr= Du =Fs=0.5, $Pr = 0.72, \delta = 2, Ec = 0.2$).
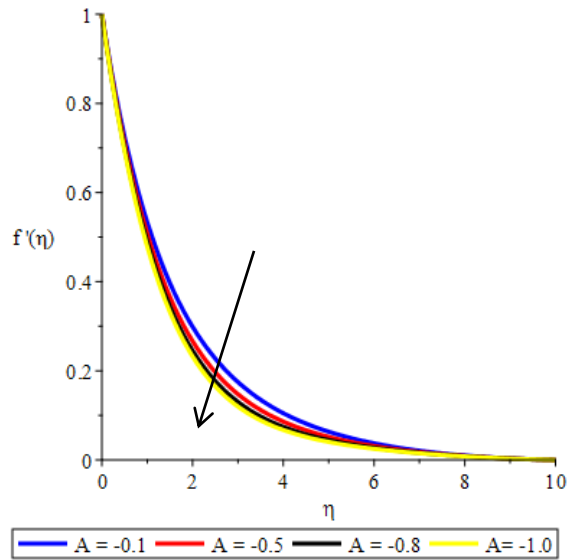

Fig14. Velocity profiles for various values of A (M=0.1, B=-0.1,Gr=Gc=5.0, Ec=0.2, Fs=Sr= Du=0.5, $\zeta = \delta = 2$)
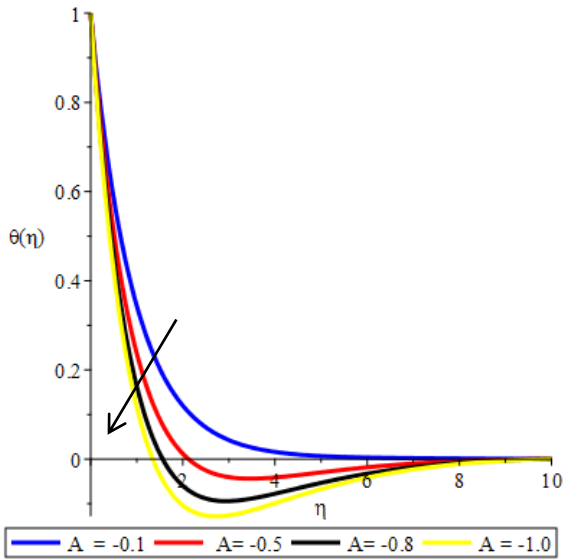
Fig15. Temperature profiles for various values of A (M=0.1, B=-0.1, Gr=Gc=5.0, Ec=0.2, Fs=Sr= Du=0.5, $\zeta = \delta = 2$)
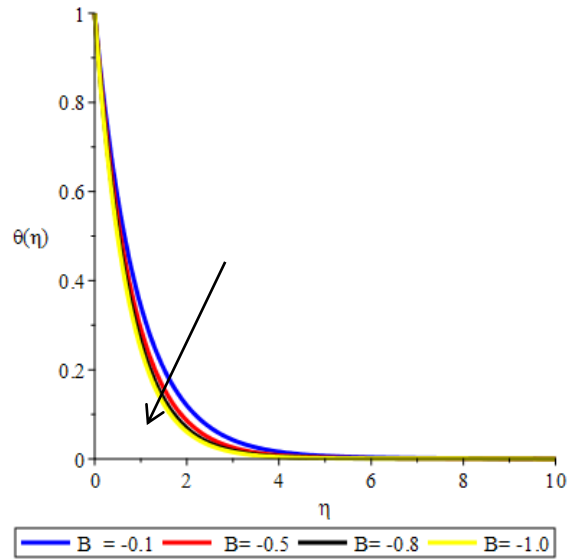

Fig17. Temperature profiles for various values of B (M=0.1, A=-0.1, Gr=Gc=5.0, Ec=0.2, Fs=Sr= Du=0.5, $\zeta = \delta = 2$)
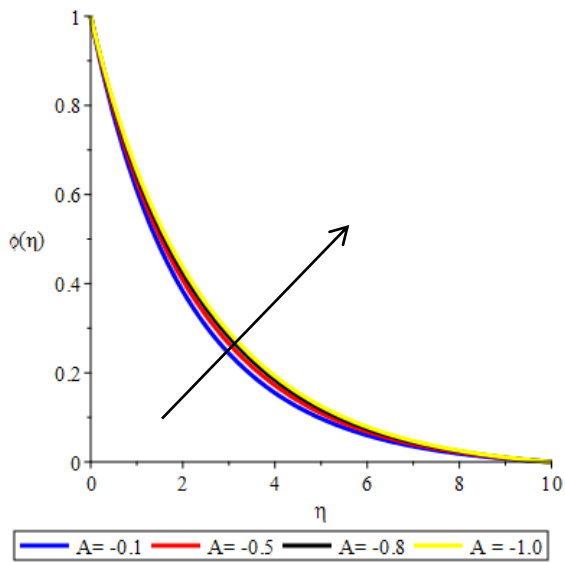

Fig16. Concentration profiles for various values of A

(M=0.1, B=-0.1, Gr=Gc=5.0, Ec=0.2, Fs=Sr= Du=0.5, $\zeta = \delta = 2$)

REFERENCES

Abo-Eldahab E. M. and El-Aziz, M. (2005). Flow and heat transfer in a micropolar fluid past a stretching surface embedded in a non Darcian porous medium with uniform free stream. *Applied Mathematics and Computation,* **162**, 881-899.

Afify, A. A. (2009). Similarity solution in MHD: Effects of thermal diffusion and diffusion thermo on free convective heat and mass transfer over a stretching surface considering suction or injection, *Commun Nonlinear Sci Numer Simulat*, **14**, 2202-2214.

Ahmadi, G. (1976). Self-similar solution of incompressible micropolar boundary layer flow over a semi-infinite plate, *Int. J. Eng. Sci*., **14**, 639-646.

Ali, M. E. (1994). Heat transfer characteristics of a continuous stretching surface, *Heat Mass Transfer*, **29**, 227-236.

Chen, C. K. and Char, M. I. /91988). Heat transfer on continuous stretching surface with suction or blowing, *J. Math. Anal. Appl*. **135**, 568-580.

Chen, J., Liang, C. and Lee, J. D. (2011)**.** Theory and simulation of micropolar fluid dynamics, *J. Nanoengineering and nanosystems,* **224**, 31-39.

Eckert, E. R. G. and Drake, R. M. (1972). *Analysis of heat and mass transfer*, McGraw-Hill, New York.

Eringen, A. C. (1964). Simple Micro fluids, Int. J. Eng. Sci. 205-217, Math. Anal. Appl. **16**, 1-18.
Eringen, A. C. (1966). Theory of Micropolar Fluids, J. Math. Anal. Appl. **16**, 1-18.
Eringen, A. C. (1972). Theory of thermo-microfluids, *Journal of Mathematical Analysis and Applications,* **38**, 480-496.

Grubka, L. J. and Bobba, K. M. (1985). Heat transfer characteristic of a continuous stretching surface with variable temperature, *Journal of Heat Transfer*, 107, 248-250.

Guram, G. S. and A. C. Smith (1980). Stagnation flow of micropolar fluids with strong and weak boundary layer flow, *Com. Maths. Appl*, **6**, 213-233.

Hassan, A. M. and El-Arabawy, (2003). Effect of suction/injection on the flow of a micropolar fluid past a continuously moving plate in the presence of radiation. *International Journal of Heat and Mass Transfer,* **46**, 1471-1477.

Hassanien, I. A., Sharmardan, A., Moursy, N. M., and Gorla, R. S. R. (1999). Flow and heat transfer in the boundary layer of a micropolar fluid on a continuous moving surface, *International Journal of numerical methods for heat & fluid flow,* **9,** 643-659.

Hassanien, I. A., El-Hawary, M, Mahmoud, M. A. A., Rahman, R. G. and Elfeshawey, A. S.   (2013). Thermal radiation effect on flow and heat transfer of unsteady MHD micropolar fluid over vertical nonisothermal stretching surface using group analysis, *Appl. Math. Engl. Ed.*, **34**(6), 703-720.

Hayat, T., Shehzad, S. A. and Qasim, M. (2011). Mixed convection flow of a micropolar fluid with radiation and chemical reaction, *Int. J. for Numer. Meth. Fluids*, **67**, 1418-1436.

Ishak, A, Nazar, R. and Pop. I. (2008). Hydromagnetic flow and heat transfer adjacent to a stretching vertical sheet, *Heat Mass Transfer*, **44**, 921-927.

Khedr, M. E. M., Chamkha, A. J. and Bayomi, M. (2009). MHD Flow of a Micropolar Fluid past a Stretched Permeable Surface with Heat Generation or Absorption, *Nonlinear Analysis Modelling and Control, 14(1), 27-40*

Kumar, L. (2009). Finite element analysis of combined heat and mass transfer in hydromagnetic micropolar flow along a stretching sheet, *Computational Materials science*, **46**, 841-848.

Kumar, B. R. (2013). MHD Boundary Layer Flow on Heat and Mass Transfer over a Stretching Sheet with Slip Effect, *Journal of Naval Architecture and Marine Engineering.10, 16-26.*

Lukaszewicz, G. (1999). *Micropolar fluids: Theory and applications,* 1st Ed., Birkhauser, Boston.

Mahmoud, M. A. A. (2011). Hydrodynamic stagnation point flow towards a porous stretching sheet with variable surface heat flux in the presence of heat generation, *Chem. Eng. Comm.*, **198**, 837-846.

Makinde, O.D. (2010). On MHD heat and mass transfer over a moving vertical plate with convective surface boundary condition, *The Canadian Journal of Chemical Engineering,* **88**(6), 983-990.

Mohamed, R. A. and Abo-Dahab, S.M. (2009). Influence of Chemical Reaction and Thermal Radiation on the heat and mass Transfer in MHD Micropolar flow over a vertical moving porous plate in a porous medium with heat generation. *International Journal of Thermal Sciences* **48**, 1800-1813.

Mukhopadhyay, S., Layek, G. C. and Samad, Sk. A. (2005). Study of MHD boundary layer flow over a heated stretching set with variable viscosity, *International Journal of Heat and Mass Transfer,* **48**, 4460-4466.

Nawaz, M., Hayat, T., and Alsaedi, A. (2012). Dufour and Soret effects in MHD flow of viscous flow between radially stretching sheets in porous medium, *Appl. Math. Mech. Engl.,* 33(11), 1403-1418.

Olajuwon, B. I., Oahimire, J. I. and Waheed, M A. (2014). Convection heat and mass transfer in a hydromagnetic flow of a micropolar fluid over a porous medium, *Theoret. Appl. Mech. TEOPM7*, **41**(2), 93-117.

Osalusi, E., Side, J. and Harris, R. (2008). Thermal-diffusion and diffusion-thermo effects on combined heat and mass transfer of a steady MHD convective and slip flow due to a rotating disk with viscous dissipation and Ohmic heating, *International Journal of Heat and Mass Transfer*, **35**, 908–915.

Pal, D. and Chatterjee, S. (2010). Heat and mass transfer in MHD non-Darcian flow of a micropolar fluid over a stretching sheet embedded in a porous media with non-uniform heat source and thermal radiation. *Commun Nonlinear Sci. Numer Simulat,* **15,** 1843-1857.

Pal, D. and Chatterjee, S. (2011). Mixed convection magnetohydrodynamic heat and mass transfer past a stretching surface in a micropolar fluid-saturated porous medium under the influence of Ohmic heating, Soret and Dufour effects, *Commun Nonlinear Sci. Numer Simulat,* **16,** 1329-1346.

Pal, D. and Mondal, H. (2011). MHD non-Darcian mixed convection heat and mass transfer over a non-linear stretching sheet with Soret-Dufour effects and chemical reaction, *International Communications in Heat and Mass Transfer,* **38,** 463-467.

Peddieson, J. (1972). An application of micropolar fluid model to the calculation of turbulent shear flow, *Int., J. Eng. Sci.*, **10**, 23-32.

Qasim, M., Khan, I. and Shafle, S. (2013), Heat and mass transfer in a micropolar fluid over a stretching sheet with Newtonian heating, *Plos One*, **8**(4), 1-6.

Rashidi, M. E. and Erfani E. (2010). A Novel analytical method to investigate effect of radiation on flow of a magneto-micropolar fluid past a continuously moving Plate with suction and blowing, *International Journal of Modeling, Simulation and Scientific Computing, 1(2), 219-238.*

Rahman, M. M. (2009). Convective flows of micropolar fluids from radiate isothermal porous surface with viscous dissipation and joule heating, *Commun Nonlinear Sci. Numer Simulat, 14, 3018-3030.*

Siddheshwar, P G. and Mahabaleshwar, U. S, (2015). Analytical solution to the MHD flow of micropolar fluid over a linear stretching sheet, *Int. J. of Applied Mechanics and Engineering*, **20**(2), 397-406.

Srinivasacharya, D. and RamReddy Ch. (2011). Soret and Dufour Effects on Mixed Convection in a Non-Darcy Micropolar Fluid. *International Journal of Nonlinear Science, 11(2), 246-255.*

Srinivasacharya, D. and Upendar, M, (2013). Soret and Dufour effect on MHD mixed convection heat and mass transfer in a micropolar fluid, *Central European Journal of Engineering, 3(4), 679-689.*

Srinivas, S., Reddy, P. B. A. and Prasad, B. S. R. V. (2013). Non-Darcian Unsteady flow of a micropolar fluid over a porous stretching sheet with thermal radiation and chemical reaction, *Heat Transfer-Asian Research*, Doi.10.1002/htj.21090, 1-15.

Subhakar, M. J. and Gangadhar, K. (2012). Soret and Dufour effects on MHD Free Convection Heat and Mass Transfer Flow over a stretching vertical plate with suction and heat sources/sink, *International Journal of Modern Engineering Research,* **2**(5), 3458-3468.

Uddin, M. T. (2011). Convective flow of micropolar fluids along an inclined flat plate with variable electric conductivity and uniform surface heat flux, *Daffodil International University Journal of Science and Technology,* **6** (1), 69-79.

Zueco, J., Ahmed, S. and Lopez-Ochon, L. M. (2014). Magneto-Micropolar flow over a stretching surface embedded in a Darcian porous medium by the numerical network method*, Arab J. Sci. Eng*., **39**, 5141-5151.